In-Depth Survey Report

Case Study: Particle Emissions from the Processes of Machining Nanocomposites

William A. Heitbrink, PhD, CIH

Li-Ming Lo, PhD

Alberto Garcia, MS

September 2013

DEPARTMENT OF HEALTH AND HUMAN SERVICES
Centers for Disease Control and Prevention
National Institute for Occupational Safety and Health

Site Surveyed: Nanomaterial manufacturing facility, eastern United States

NAICS Code: 325199

Survey Date: May 2012

Survey Conducted by: William A. Heitbrink, NIOSH/DART/EPHB

Li-Ming Lo, NIOSH/DART/EPHB

Alberto Garcia, NIOSH/DART/EPHB

Employer Representative Contacted: Jessica Ravine, Buckeye Composites

Contractor Representative: None

Disclaimer

Mention of any company or product does not constitute endorsement by NIOSH. In addition, citations to websites external to NIOSH do not constitute NIOSH endorsement of the sponsoring organizations or their programs or products. Furthermore, NIOSH is not responsible for the content of these websites. All Web addresses referenced in this document were accessible as of the publication date.

Table of Contents

Abstract

This case study was completed in response to a company request to investigate the release of carbon nanotubes (CNTs) during cutting and sanding of composite panels containing CNTs. To evaluate the release of CNTs, a ventilated enclosure was built to capture and mix the emissions from sanding and cutting composite panels. The ventilation system consisted of a partial enclosure around the band saw, a metal duct, and a clean air machine that provided air flow and filtration. The volumetric air flow through the test system was 1,072 cubic feet per minute (cfm), with a hood face velocity of 197 feet per minute (fpm). The panel sanding and cutting was performed inside the hood face to reduce workers' dust exposure and to capture emissions for characterization. The process emissions were well mixed because of the inclusion of a baffle and a 90° elbow upstream of the sampling location. A portable air exhaust system exhausted air through the enclosure, the 90° elbow, and the 12-inch-diameter duct.

Process emission rates were computed on the basis of air flow and concentration. To determine dust concentrations, air samples were collected 15 duct diameters from the elbow. It was expected that at this location the emissions would be well mixed, and that samples collected from the center core of the duct would be representative. The number concentration of particles in the range of 7 to 560 nanometers (nm) was measured with a Fast Mobility Particle Sizer (TSI Inc., Shoreview, MN). Isokinetic sampling was conducted to obtain samples for determining the following:

- particle number concentrations (from 0.5 to 20 micrometers, μm), by means of an Aerodynamic Particle Sizer (TSI Inc., Shoreview, MN),
- aerosol mass concentration, based upon light scattering, by means of an aerosol photometer,
- elemental carbon in a filter sample, per NIOSH Method 5040, and
- fiber concentration in a filter sample, measured by transmission electron microscopy (TEM), per NIOSH Method 7402.

Four different composite panels were tested:
- panel A, an IM7 graphite fiber/BMI (bismaleimide) composite panel,
- panel B, an IM7 graphite fiber/epoxy composite panel,
- panel C, an IM7 graphite fiber/epoxy composite panel with a carbon-based nonwoven mat (fiber diameter of 7.5 μm) as a surface ply,

- panel D, an IM7/epoxy panel with multiwalled CNT–coated carbon-based nonwoven mat as a surface ply.

Cutting the composite with the band saw did not result in the detection of CNTs or other fibers by TEM. In addition, the presence of CNTs did not greatly increase measured amounts of elemental carbon, aerosol mass, and aerosol number. However, the number concentration of particles smaller than 560 nm exceeded 10^5 particles per cubic meter (cm^3), as compared with background concentrations, which averaged 1.09×10^4 particles/cm^3. The calculated emission rates per volume of material removed during cutting ranged from 70 to 230 milligrams per cubic meter (mg/cm^3) of cut volume (the product of blade diameter, panel thickness, and cut length) and from 2.95×10^{13} to 6.72×10^{14} particles/cm^3 of cut volume. The high number concentration and emission rates may have been caused by the formation of nano-aerosols generated by frictional heating and did not appear to be elevated by the presence of CNTs.

Sanding the composite panel D, which contained CNTs, generated fiber emission rates of 1.9×10^8 and 2.8×10^6 fibers per second. No measurable fiber concentrations were generated from panels that contained graphite and carbon fibers (panels A, B, and C). The particle number concentration in the duct was about 10^3 particles/cm^3; this may be largely attributed to the carbon brushes that are part of the sander's motor. Mass emission rates were between 0.01 and 0.36 milligrams per second (mg/sec). However, the pressure applied to the sander by the worker was not controlled, and this may have caused a wide range in the mass and fiber emission rates.

The ventilated enclosure used in this study effectively contained the emissions from panel cutting and sanding processes. Because sanding composites containing CNTs resulted in noticeable emissions of fibers, careful and aggressive control of exposure to CNTs is recommended. These emissions could probably be controlled by either a conventional local exhaust ventilation hood or a high-velocity, low-volume ventilation system. Local exhaust ventilation can also be used to capture and collect the aerosol and debris generated by the band saw.

Introduction

Background

Researchers in the Engineering and Physical Hazards Branch (EPHB) of the National Institute for Occupational Safety and Health (NIOSH) are focused on hazard control, specifically the control of worker exposure to air contaminants. This report addresses the characterization of emissions generated by machining composites containing engineered nanomaterials. Machining operations may release engineered nanomaterials into the workplace. Potential risks associated with nanoparticle exposure from engineered nanomaterials have been reported following toxicological research [Buzea et al. 2007; European Agency for Safety and Health at Work 2009; ISO 2008; Safe Work Australia 2009a]. Consequently, workplace controls have been recommended to prevent or minimize exposure to engineered nanomaterials [Safe Work Australia 2009b]. EPHB is conducting research to evaluate controls and develop appropriate recommendations with regard to nanomaterials. This study was funded by the NIOSH Nanotechnology Research Center (NTRC).

The site that is the subject of this report produces a paper used in the production of structural composites. These composites may include single, double, and/or multiwalled carbon nanotubes (MWCNTs), carbon nanofibers, and/or other nanomaterials, along with carbon fibers and polymer resins [Traceski 1999; Zimmer et al. 2012]. Ultimately, the structural composite materials that contain these nanomaterials will need to be cut, drilled, or sanded during production, maintenance, or repair operations. The extent to which these operations release nanomaterials is not understood. This study addresses two objectives:

1. Evaluate whether cutting with a band saw or sanding with an orbital sander can release nanomaterials into the workplace air.
2. Quantitatively evaluate the emission rate of these particles so that exposures can be estimated for various ventilation scenarios.

Potential Health Effects

There are no published study reports on adverse health effects in workers producing or using CNTs or carbon nanofibers (CNFs). The concern about worker exposure to CNTs or CNFs arises from results of animal studies. Studies in rodents have shown an equal or greater potency of CNTs,

compared with other inhaled particles known to be hazardous to exposed workers (ultrafine carbon black, crystalline silica, and asbestos), in causing adverse lung effects such as pulmonary inflammation and fibrosis [Shvedova et al. 2005]. Early onset and persistence of pulmonary fibrosis were noted in CNT-exposed animals in short-term and subchronic studies [Pauluhn 2010; Porter et al. 2010; Shvedova et al. 2005], and reduced lung clearance was noted in rats exposed to low mass concentrations of CNTs [Hubbs et al. 1997]. Findings of acute pulmonary inflammation and interstitial fibrosis have also been observed in mice exposed to CNFs [Hubbs et al. 1997; Kisin et al. 2010]. In addition, the long, thin structures of some CNTs and CNFs dimensionally resemble asbestos fibers, and MWCNTs have been observed to migrate from pulmonary alveoli to the pleura tissue, the same site in which malignant mesothelioma can develop due to asbestos exposure [Hubbs et al. 1997; Kisin et al. 2010; Porter et al. 2010]. However, the relationship between health effect and fiber dimensions (such as diameter and length) has not been established [Castranova et al. 2012; Murashov and Howard 2011; Nagai et al. 2011]. Though additional research is needed to further elucidate the mechanisms of biological responses to CNTs and CNFs, these findings of adverse respiratory effects in animals indicate the need for precautionary measures to limit the risk of occupational lung disease in workers with potential exposure to CNTs and CNFs.

Applications for Carbon Nanotubes and Carbon Nanofibers

CNTs and CNFs are currently used in numerous industrial and biomedical applications, including electronics, lithium-ion batteries, solar cells, super capacitors, reinforced plastics, micro-fabrication conjugated-polymer activators, and biosensors; enhanced electron-scanning microscopy imaging techniques; and pharmaceutical/biomedical devices for bone grafting, tissue repair, drug delivery, and medical diagnostics. CNTs and CNFs can be encountered in facilities ranging from research laboratories and production plants to operations where they are processed, used, disposed, or recycled. The extent of worker exposure to CNTs and CNFs is poorly understood, but workplace exposure measurements of CNTs have shown potential for worker exposure [Bello et al. 2008; Evans et al. 2010; Han et al. 2010; Lee et al. 2010; Methner et al. 2009; Methner et al. 2007; Tsai et al. 2009].

Machining of Composites Containing Nanomaterials

During fabrication of structures from composites containing nanomaterials, the composites are subjected to common machining operations such as cutting, sanding, grinding, and hole drilling. Nanomaterials may be released from the composites under these operations. The cutting, sanding, and grinding can cause the generation of very high concentrations of ultrafine particles ($>10^5$ particles/cm^3) [Bello et al. 2008; Bello et al. 2010; Bello et al. 2009; Kuhlbusch et al. 2011; Methner et al. 2012]. CNTs or CNFs may be released as bundles of agglomerated nanomaterials or as individual fibers [Bello et al. 2010; Cena and Peters 2011; Methner et al. 2012; Schlagenhauf et al. 2012]. Mechanical operations can involve frictional heating that may cause the generation of ultrafine aerosol, with particle sizes smaller than 100 nm [Stabile et al. 2012]. During mechanical operations involving scratching, cutting, and sanding, nanoparticle and ultrafine aerosol releases were reportedly related to the energy transported to the surface [Gheerardyn et al. 2010]. The amount of such energy is a function of the coefficient of friction, the force vector perpendicular to the surface, and tool speed. Ultimately, the mechanical power of the machining operation is converted to heat, which can increase tool and substrate temperature [Malkin and Guo 2007]. According to studies of machining operations involving carbon-reinforced composites, tool temperatures can reach 287–350°C, and scorch marks are observed [Chang et al. 2011; Weinert and Kempmann 2004]. In structural composites involving graphite fibers cured into epoxy resins, thermal decomposition has two phases, at 280°C and 340°C [Chen 1997; McShane et al. 1999]. Increasing the CNT content of an epoxy composite from zero to 2% promoted the threshold for thermal decomposition from 339°C to 378°C [Chen et al. 2008]. Temperatures >400°C are reported to cause thermal decomposition of some CNTs [Hsieh et al. 2010]. Clearly, frictional heating of the composites can increase surface temperatures such that thermal decomposition of the composite matrix could release CNTs.

Published Regulations

OSHA has not published an occupational exposure limit (OEL) for CNTs [Occupational Safety and Health Adminstration 2013]. However, some draft and provisional exposure limits are listed in Table 1. The available toxicological information regarding health effects of CNT exposure resulted in the development of a NIOSH Current Intelligence Bulletin (CIB) specific to CNTs and CNFs. The NIOSH CIB on CNTs proposes a recommended exposure limit (REL) of 1 microgram per cubic meter (μg/m^3) elemental carbon as a

respirable mass 8-hour time-weighted average (TWA) concentration [NIOSH 2013]. Others have recommended OELs for engineered nanomaterials, including CNTs, and these are listed in Table 1.

The provisional or suggested exposure limits in Table 1 are nonspecific, and extraneous sources can affect these measurements. Background air pollution and industrial processes can generate particles the same size as engineered nanomaterials. A particle number concentration of 20,000/cm^3 in an urban environment is routine [Morawska et al. 2008; Shi et al. 2001; Stanier et al. 2004]. In the ambient environment, elemental carbon concentrations are reportedly as high as 5 μg/m^3, with a mean of 0.6 μg/m^3 and a standard deviation of 0.7 μg/m^3 [Yu et al. 2004]. Advanced composites used in the aerospace industry commonly contain carbon or graphite fibers [Traceski 1999]. Furthermore, there is considerable interest in combining micrometer-sized carbon fibers with CNTs to enhance the performance of advanced composites [Zimmer et al. 2012]. In applying these limits, there is a need to evaluate whether the exposure measurement is caused by extraneous processes, background air pollution, or engineered nanomaterials [Van Broekhuizen et al. 2012; Van Broekhuizen and Dorbeck-Jung 2012].

Table 1. Provisional or draft exposure limit recommendations for engineered nanomaterials

Description	Limit	Source of Recommendation
Baytubes® (multiwalled CNTs)	50 μg/m^3	[Bayer MaterialScience 2010]
Carbon nanotubes measured as respirable elemental carbon	1 μg/m^3 as an 8 hour TWA	NIOSH Current Intelligence Bulletin 65 [NIOSH 2013]
Nanocyl CNTs	2.5 μg/m³	Nanocyl case study [Nanocyl 2009]
Biopersistent granular nanomaterials in the range of 1–100 nm with density >6000 kg/m^3	20,000 particles/cm^3	Nano reference value [Van Broekhuizen et al. 2012; Van Broekhuizen and Dorbeck-Jung 2012]
Biopersistent granular and fiber-form nanomaterials in the range of 1–100 nm with density <6000 kg/m^3	40,000 particles/cm^3	
Rigid, biopersistent nanofibers (including CNTs) for which effects similar to those of asbestos are not excluded.	0.01 fibers/cm^3	

Materials and Methods

This study was conducted to obtain insight about emissions from downstream mechanical processes that might be conducted on composites containing nanomaterials. Material samples were obtained from a specific user/client. Specifically, the emissions generated by the following operations were studied:

1. Cutting the composite with a band saw (Delta Model 20, Delta Power Equipment Company, Anderson, SC). This band saw (Figure 1) has a nominal blade speed of 5100 fpm and was used with a 151-inch-long blade that resembled the fine-tooth blade of a hack saw. The band saw is driven by the bottom wheel. The table was approximately 2 feet square. The blade width was 0.03 inches.
2. Sanding with an orbital sander (Model S652D, Ryobi Technologies, Anderson, SC). The sander is operated in orbital motion with the nominal speed at 14000 rotations per minute (RPM), and its orbit diameter is 1/16 inches. It fits 1/4 sheet sandpapers of different size grits depending upon finishing requirements. In this study, we used the dust bag assembly to remove dust as normal operation, rather than attached the sander to a vacuum.

To conduct this testing, a ventilation system was assembled including an enclosing hood, about 20 feet of duct, and a portable air exhaust system. The enclosing hood and mixing plenum behind the hood were fabricated from plastic pipe, 6-mil vapor barrier, and duct tape. The air exhaust system (i.e., negative air machine) moved and filtered contaminated air before discharging the air back into the workplace. The air in the duct was sampled isokinetically with an integrated filter and aerosol instrumentation to determine the in-duct concentration. Air samples were collected on filters to determine the concentration of elemental carbon and fiber number concentrations in the duct, on the worker, and at a background location. Emission rate was computed as the product of air flow and in-duct concentration. This ventilation system was constructed so that all of the emissions would be captured and transported to the sampling location. Sanding of the composite panels was performed on the band saw table. An important design objective was to prevent worker exposure to the emissions released by the cutting and sanding operations.

Figure 1. Bandsaw with access doors open.

Aerosol Measurements

Direct-reading instruments used in real-time mode can help identify major emission sources and assess the efficiency of control measures in the manufacturing workplace. They provide continuous measurements of concentrations, which can be correlated with the specific production equipment and work processes [Ham et al. 2012]. Because of the lack of established exposure criteria, measurements of number and mass concentrations and size distributions of nanomaterials are needed [Mark 2007]. The instruments used to measure particle concentrations in this survey (all manufactured by TSI, Inc., Shoreview, MN) were the Fast Mobility Particle Sizer (FMPS) spectrometer, Aerodynamic Particle Sizer (APS) spectrometer, and DustTrak aerosol monitor (Table 2). The FMPS and the APS were used exclusively for in-duct sampling. The APS and FMPS provide number concentrations expressed as particles/cm^3. Mass

concentrations can be estimated on the assumption that the aerosol particles are spherical with a density (ρ) of 1 gram/cm^3. The following formula was used to calculate the mass concentration (C_m) from the number concentration ($C_{n,i}$) for each channel i of j channels and the particle diameter (d_i):

$$C_m = \sum_{i=1}^{j} \frac{\pi}{6} d_i^3 \rho \, C_{n,i}$$ ....Equation 1

The respirable mass of aerosol (C_{resp}) can be computed with use of a factor, $f_{resp,i}$. This term is the fraction of the aerosol that is respirable in channel i. The formula to compute this term is documented in Appendix C of the ACGIH list of Threshold Limit Values for chemical substances [ACGIH 2012].

$$C_{resp} = \sum_{i=1}^{j} \frac{\pi}{6} d_i^3 \rho \, f_{resp} C_{n,i}$$ ....Equation 2

All of the mass emissions from the FMPS were assumed to be respirable. The mass fraction of respirable aerosol was computed as C_{resp}/C_m.

Table 2. Direct-reading instruments used in this study

Instrument*	Metrics	Specifications
FMPS (Model 3091)	Number	(1) Determines number size distributions with an array of electrometers (2) Size range from 5.6 to 560 nm (3) As particle size increases from 5.6 to 560 nm, maximum number concentration decreases from 10^7 to 10^5 particles/cm^3 and minimum detectable concentration, for a 1-second sample, decreases from about 300 to 2 particles/cm^3.
APS (Model 3022)	Number	(1) Measures number size distributions with light-scattering technique (2) Size range from 0.5 to 20 µm (3) Determines maximum useful concentration by the simultaneous presence of 2 or more particles in the detection volume. This is termed coincidence error and can cause undercounts. For 0.5-µm particles, the coincidence error is <2% at 1000 particles/cm^3. For 10-µm particles, the coincidence error is <6% at 1000 particles/cm^3.
DustTrak (Model 8533)	Mass	(1) Single-channel basic photometric instrument (2) Size range from 0.1 to ~15 µm (size segregated mass fractions for PM_1, $PM_{2.5}$, respirable, PM_{10} and total) for concentration range from 0.001 to 150 mg/m^3

* All manufactured by TSI, Inc., Shoreview, MN.

Integrated Air Samples

Air samples to determine the airborne mass concentration of elemental carbon were collected on 25-mm-diameter, open-face quartz fiber filters (QFFs) and analyzed according to NIOSH NMAM 5040 for Elemental Carbon (Diesel Particulate) using Evolved Gas Analysis (EGA) with a thermal-optical

analyzer [NIOSH 2003]. Seven media blanks were processed for determining the limit of detection (LOD; 0.08 µg/filter) and the limit of quantitation (LOQ; 0.25 µg/filter). All sample results for the 25-mm cassettes are based on an effective sampling area of 3.46 square centimeters.

Alongside each mass-based air sample, an additional air sample was collected on a 25-mm-diameter, open-face mixed cellulose ester (MCE) filter and analyzed for CNTs by transmission electron microscopy (TEM) with energy-dispersive spectroscopy (EDS) in a manner similar to NIOSH NMAM 7402 [NIOSH 1994]. Three 3-mm copper TEM grids from each sample were examined at low magnification to determine loading and preparation quality. The counting protocol included the following stopping rules: 40 grid openings or 100 structures. TEM with EDS provides an indication of the relative abundance of nanostructures per cm^3 of air, as well as other characteristics such as size, shape, chemical composition, and degree of agglomeration. These samples were collected at a flow rate of 4 liters per minute (L/min) with a Universal Aircheck Sampler, Model 224-PCXR (SKC, Eighty-Four, PA).

The filter samples were collected in the duct, on the worker, in the enclosure just downstream of the sanding or sawing operation, and at a background location. A background sample was taken during each day of the study. This sample was collected behind the enclosure, some 30 feet from the air exhaust system.

Test System Description and Commissioning

Test Setup

The clockwise motion of the band saw blade may drag dusty air into the internal spaces of the band saw, which is below the band saw's table. This saw also has an exhaust take-off located beneath the table, which was closed off with duct tape (Figure 1). Thus, the entire back of the band saw was included in the enclosure so that dust from this chamber was contained for the emission measurement (see Figures 2-4). As shown in these figures, the enclosure was constructed from PVC pipe and 6-mil polyethylene.

The face of this hood was sized to allow the operator access to the saw blade and the power buttons, which were just inside the hood (see Figure 3). Located downstream of the test hood, a portable air exhaust system (NOVAIR 200, Novatek Co., Buxton, PA), which included a fan and High Efficiency Particulate Air (HEPA) filters, was used to exhaust suspended airborne particles. The exhaust air flowed across the table and through one

of three horizontal slots cut into the vapor barrier that formed the air distribution plenum in the back of the hood (Figure 4). Behind this air distribution plenum, a baffle constructed of cardboard was used to mix the air. Two 1 × 38–inch vertical slots were cut out of the cardboard about 1.5 inches from the side of the cardboard baffle. This was done to create turbulence to mix the aerosol.

This test system was intended to promote mixing, so that a single point would yield a representative sample of the aerosol in the duct. The space between the baffle and the connection to the 12-inch diameter duct (see Figure 2) would cause the formation of large-scale eddies, leading to mixing [McFarland et al. 1999]. Elbows also cause turbulence and mixing. The sampling location was 15 duct-diameters downstream of the elbow (see Figure 5), which was expected to ensure adequate mixing of the aerosol [Hampl et al. 1986].

Top half of frame, and space between PVC and band saw is wrapped in 6 mill polyethylene vapor barrier which forms an enclosure

33

baffle →

Connection to 12 inch Diameter duct

62

39

Side view

81

79

23

52

Band saw

Enclosure opening, average face velocity 197 fpm

26

4

46

35

Front view

Note: All dimensions are in inches.
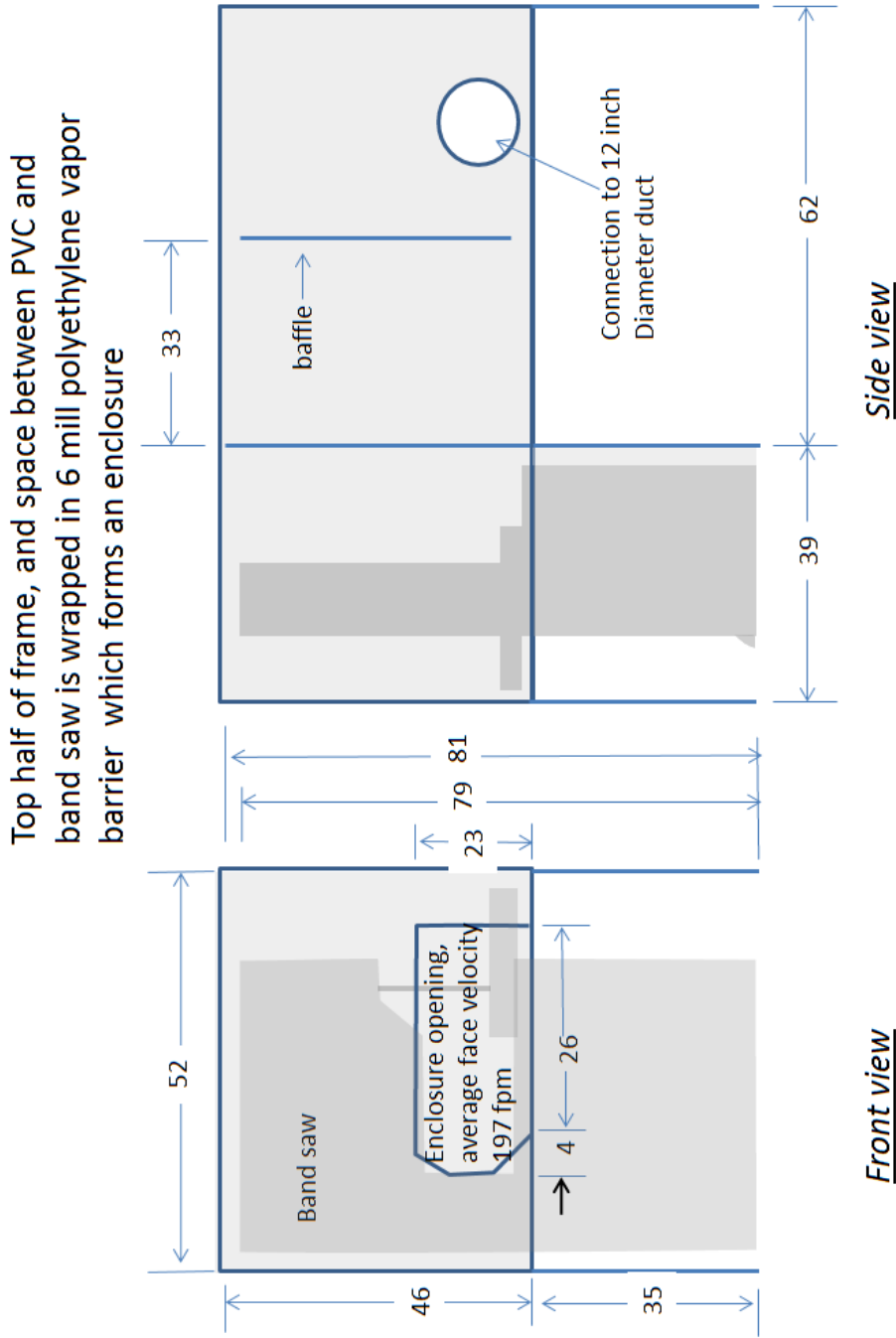
Figure 2. Drawing of enclosure around band saw.

Figure 3. Front view of enclosure around band saw.

Figure 4. Side view of enclosure around band saw. The hole in the enclosure above the support stand is where the elbow was inserted into the enclosure.
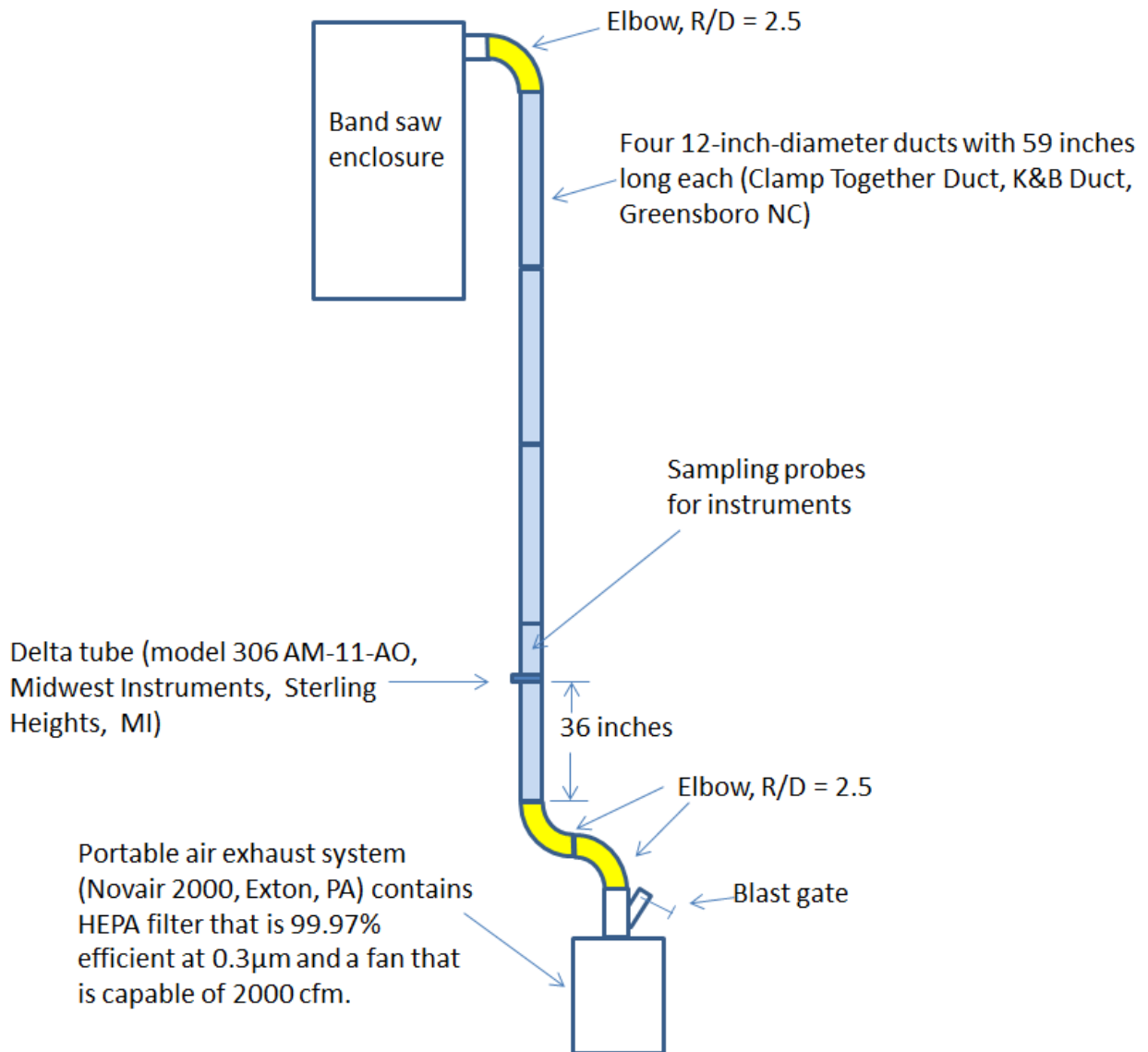
Figure 5. The connecting duct between the enclosure and the portable air exhaust system.

Exhaust Air Delivery

Figure 5 shows the configuration of the duct system connecting the enclosure to the negative air machine. The duct was constructed from 4 straight segments of 12-inch-diameter Clamp Together Duct (K&B Duct, Greensboro, NC), 3 elbows, and 1 branch connection. The branch connection just upstream of the air exhaust system mixed air from the duct system and an 8-inch branch. An adjustable blast gate was placed on this branch connection, and the blast gate was adjusted to obtain a duct centerline velocity of 1400 fpm, as measured by the hot wire anemometer (Velocicalc Plus, Model 8386A, TSI, Shoreview, MN). Two 10-point pitot tube traverses were conducted horizontally and vertically to measure airflow, by means of procedures documented elsewhere [ACGIH 2007]. Hood face velocities were measured with the hot wire anemometer.

Isokinetic Sampling from Duct

Instrument and integrated filter samples were collected in the fourth duct segment (Figure 5), which was just upstream of the connection between the duct and the air exhaust system. The sampling probe nozzles were sized so that the inlet velocity matched the duct center-line velocity of 1400 fpm. Further details of the connection between the instruments and the duct are shown in Figure 6. The filter sampling probes were fashioned by the fitting of a brass nozzle onto an open-face filter. The nozzle was fabricated from brass shim stock that had a thickness of 0.3 mm. The inlet diameter was 3.5 mm, which expanded to 25 mm in a distance of 33 mm, as measured by a caliper. The inlet angle was estimated to be 15°. The sampling rate was 4 L/min to obtain an inlet velocity of 1400 fpm.
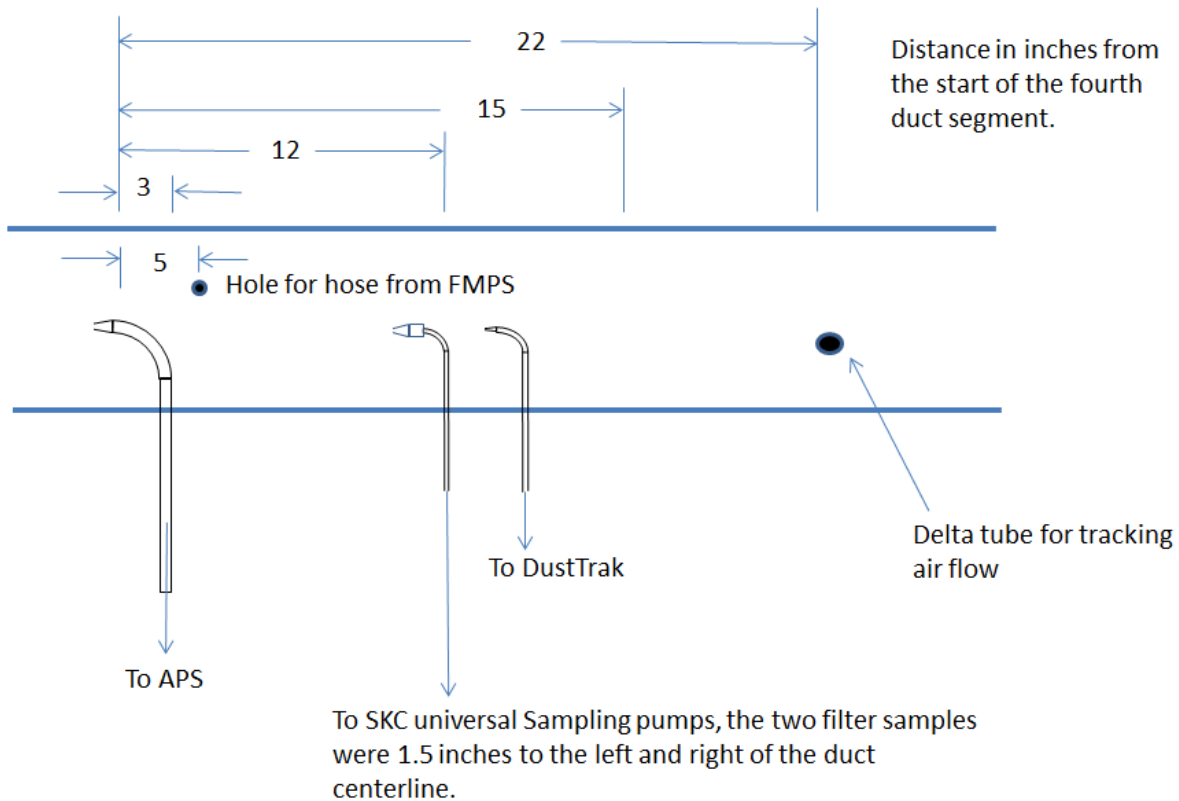
Figure 6. Details of connections between instrumentation and duct.

The FMPS sampled air through a hose inserted into the duct at the location shown in Figure 6. As particle size increases above 0.56 µm, isokinetic sampling is needed so that particle inertia does not affect sampling efficiency. The sampling nozzles for the filter samples, the APS, and the DustTrak were sized for an air velocity of 1400 fpm. As shown in Figure 6, the APS and DustTrak sampled through a nozzle which expanded to the tube diameter listed in Table 3. The tubing diameters were chosen to keep the flow in the tubing laminar so that turbulent deposition would not occur in the elbow or in the straight sections of tubing [Brockman 2001]. However, gravitational settling losses in the nozzle were unavoidable. The overall transmission efficiency (i.e., aerosol penetration through the nozzle) was estimated by calculating the product of the gravitational and inertial transmission efficiencies [Brockman 2001], and the results of these calculations are shown in Table 3.

Table 3. Sampling parameters for APS, DustTrak, and filter samples.

Parameter	DustTrak	APS	Filter samples
Sampling rate, L/min	3	5	4
Inlet diameter, cm	0.30	0.39	0.35
Inlet length, cm	2.00	5.00	3.3
Tubing diameter, cm	0.95	1.92	Not relevant
Tubing Reynolds number	445	353	
Elbow R/D	4	7	
Transmission efficiency estimate at particle diameter, μm	DustTrak	APS	Filter samples
1	0.997	0.997	0.997
5	0.96	0.95	0.95
10	0.89	0.88	0.88

Test Materials

Cutting and sanding were performed on 12 × 12–inch panels, which were cut in half on the band saw. Half of each panel was used to study aerosol generated by cutting on the band saw, and the other half was used to study aerosol generated by sanding. The test panels all contained graphite fiber (IM7, Hexcel Corp., Stamford, CT), dispersed throughout the panels. This fiber's filament diameter is 5.2 μm. Information for each test panel is shown as follows:

Panel A: an IM7 graphite fiber/BMI (bismaleimide) composite panel intended for practice to work out test procedures. The results from these panels are included for complete documentation of results.

Panel B: an IM7 graphite fiber/epoxy composite panel.

Panel C: an IM7 graphite fiber/epoxy composite panel with carbon-based nonwoven mat as a surface ply. The mat has a fiber diameter of 7.5 μm.

Panel D: an IM7/epoxy panel with MWCNT-coated carbon-based nonwoven mat as a surface ply. This mat was the same used in panel C. The mat was coated with M-grade MWCNTs and binder. The M-grade MWCNTs (Buckeye Composites, Kettering, OH) are typically about 6.5% by weight residual iron catalyst, with an average diameter of 50 nm and an average length of 1 mm.

Calculation of Emission rate

For composite cutting, the results are presented as a concentration and emission rate. To compute emission rate, the concentration increase, *ΔC*, is computed as the difference between the concentration during the sampling time and the average concentration measured before the composite was cut. Because the panel thicknesses and cut length varied, concentrations are not directly comparable. The emission rates, ER_V, are normalized on the basis of volume of composite cut (V_c), air flow (*Q*), and sampling time (*t*). The blade thickness was 0.03 inches, as measured by a caliper. The formula for computing emission rate is:

$$ER_V = \frac{\Delta C\, Q\, t}{V_c}$$ ....Equation 3

Where

$V_c = (blade\ thickness) \times (length\ of\ cut) \times (panel\ thickness).$

For the aerosol instrumentation, *ΔC* is computed:

$$\Delta C = [concentration\ during\ cutting\ or\ sanding \\ - average\ concentration\ during\ the\ prior\ 5\ minutes].$$

For the filter samples collected in the duct, the concentration increase is computed as the difference between the in-duct concentration and the background concentration measured near the back of the enclosure.

Emission rate has dimensions of fibers, milligrams, or particles per volume of material cut (cm³), depending upon the instrument or sampling method.

For sanding the composite, the results are presented as the measured concentration and the calculated emission rate, ER_t, that is based upon the sanding time. The concentrations are computed on the basis of actual sampling time. For the sander, emission rate was computed on the basis of sanding time:

$$ER_t = \frac{(sampling\ time\ )Q\Delta C}{sanding\ time}$$ ....Equation 4

In this formula, ΔC is the concentration increase, as described earlier. This corrects for varying background concentrations.

Test Procedures

Before data collection, the times on all of the computers and instruments were synchronized. Data collection occurred on 2 days. At the start of each day, background samples for elemental carbon and fibers were collected outside of the test enclosure (about 30 feet from the discharge of the clean air machine). These samples provide insight into the ambient concentrations in the plant. With a sampling position just above the middle of the enclosure's opening (Figure 3), the DustTrak was used to monitor the aerosol mass concentration close to the worker's breathing zone. The DustTrak was set on the floor and a 7-foot length of 0.19-inch-diameter conductive hose transported the air sample to the instrument. The aerosol instruments logged concentrations every second during the entire data collection effort for the day. A caliper was used to measure the thickness of each composite panel and the thickness of the band saw's blade.

Panel Cutting

Before using the band saw to cut composites, we characterized the aerosol emissions from the band saw itself. The band saw was operated for a period of 10 minutes without cutting composites. The aerosol instrumentation measured the in-duct concentration downstream of the band saw at the sampling locations shown in Figure 5. However, filter samples were not collected, because these emissions appeared to be minimal.

There were two sessions during which the composite panels were cut. The total length of cut differed during the two sessions. During the first session, the test panel was cut in half. Half of the panel was reserved for the sanding experiments. Then, the other half of the panel was repeatedly cut, resulting in 6-inch-long pieces of composite that were discarded. The cuts were along the 6-inch length of the half panel. For panels A, B, and C, there were 11 six-inch-long cuts. For panel D, which appeared to be creating more dust, there were 5 six-inch-long cuts. The actual sampling time was about 1 minute longer than the cutting time to allow the concentration pulse to pass the in-duct isokinetic sampling location.

During the second cutting session, a single 6-inch cut was made from a remaining piece of composite. This second session was used to provide a lightly loaded sample for TEM analysis. Overloaded filters are unsuitable for counting by TEM.

Panel Sanding

During the sanding experiments, the Ryobi sander with fresh (100-grit) sandpaper was used on the 12×6 inches composite panel. Similar to routine operation, holes were made in the sandpaper with a paper punch to collect dust in the dust bag attached to the sander. The worker held the composite in place with one hand and used the sander with the other hand. The start and stop times for sanding were recorded and used to estimate the concentration. The actual sampling time was about 1 minute longer than the sanding time to allow the concentration pulse to pass the in-duct isokinetic sampling location. For panel D, two panels were tested (panels D1 and D2).

During the testing of panel A, there were numerous experimental problems and changes. The data from testing this panel were included for the sake of report completeness, although they were not considered in the data analysis. The overall sampling duration was 30 minutes. The sanding times and activities were as follows:

1. For 261 seconds, sanding with 220-grit sandpaper without holes.
2. For 213 seconds, sanding with 100-grit sandpaper with holes for drawing air through the small bag pictured in Figure 7. The computer controlling the FMPS stopped working during this run, and the run was repeated.
3. For 179 seconds, sanding with 100-grit sandpaper with holes drawing air through the small bag.

After conducting the testing, we learned that the sander contained carbon brushes, a reported source of extraneous aerosol generation [Heitbrink and Collingwood 2005; Koponen et al. 2009; Szymczak et al. 2007; Trakumas et al. 2001]. In electric motors, carbon brushes, which are essentially sticks or blocks of graphite, rub against the rotating commutator to complete the power circuit. This creates dust due to abrasion and, perhaps, arcing. The heat and aerosol are discharged through ventilation holes in the sander's handle. To evaluate the emissions from the sander, the exhaust duct and air cleaner were assembled as shown in Figure 5. The sander was positioned at the inlet to the elbow, as shown in Figure 7. The blast gate was set so that the air velocity in the center of the inlet duct was 1400 fpm, as measured by the hot wire anemometer. A 10-point tube traverse was conducted to obtain the airflow. The air flow was 944 cfm and the air velocity near the APS's sampling probe was 1300 fpm, indicating the velocities were sub isokinetic. The sander was operated for four 10-minute periods, and the aerosol instrumentation was used to characterize the emissions. The concentration increase was computed as described in the section for the band saw. Emission rates units are particles, fibers or mg of aerosol per second of sanding.

Figure 7. Positioning of the sander at the inlet to the duct.

Results

Ventilation Measurements

The ventilation measurements made to characterize the performance of the test system (Figure 5) are summarized in Table 4. The hood face velocity at the inlet was 197 fpm (see Figure 2 and Figure 3). At this location, qualitative flow visualization with smoke tubes did not reveal the presence of eddies that might transport air contaminants out of the hood. The band saw blade was located about 14 inches inside the enclosure. When the band saw was operated, the emissions appeared to be contained within the test system. During sanding, the test panels were located near the inlet to the enclosure. The total air flow was 944 cfm during laboratory testing.

Table 4. Ventilation parameters for test system

Location	Parameter	Measured by	Average (fpm)	Standard deviation (fpm)
–	Desired air velocity near probes (for isokinetic sampling)	Hot wire anemometer	1400	–
Field	Face velocity at enclosure opening (4.15 ft^2)	Hot wire anemometer	197 (819 cfm)	20
	Air velocity near probes	Pitot tube	1366 (1072 cfm)	90
Laboratory	Air velocity near probes	Pitot tube	1203 (944 cfm)	130

Worker Exposure Measurements at Hood Face

The aerosol photometer concentration measurements were unaffected by the operations conducted in the enclosure (Table 5). Apparently, the ventilated enclosure contained the emissions with minimal leakage.

Table 5. Average DustTrak concentrations measured above hood face in breathing zone.

Operation	Background (mg/m^3)	Concentration During Operation (mg/m^3)
Multiple cuts with band saw		
Panel A	0.15	0.18
Panel B	0.07	0.08
Panel C	0.08	0.09
Panel D	0.08	0.10
One cut with band saw		
Panel A	0.05	0.06
Panel B	0.05	0.05
Panel C	0.05	0.06
Panel D	0.06	0.06
Sanding		
Panel A	0.05	0.05
Panel B	0.04	0.05
Panel C	0.05	0.05
Panel D1	0.06	0.07
Panel D2	0.05	0.05

Emissions from Band Saw Cutting

To compute emission rate as shown in Equation 3, the values of V_c are presented in Table 6. In this table, the panel thicknesses are not uniform and computation of an emission rate is an adjustment for the non-uniform thickness of the panels and the varying lengths of cut. For the first session, the value of V_c ranged from 2.3 to 6.7 cm^3.

Table 6. Cut dimensions for the first and second test series

Composite	Panel thickness (inches)	Number of 6-inch cuts during 1st test series	Volume of cut, cm^3, for 1st test series	Length of cut, inches, for 2nd test series	Volume of cut, cm^3, for 2nd test series
Panel A	0.131	11	5.023	6.19	0.40
Panel B	0.081	11	3.106	6.00	0.24
Panel C	0.177	11	6.787	5.69	0.49
Panel D	0.111	5	2.292	6.63	0.36

As described in the procedures section, there were two test series. The purpose of the second session was to collect samples for TEM without overloading sampling filters. The V_c was used to normalize the concentration data and compute emissions per volume of cut. The operation of the band saw was uneventful until the blade broke while cutting panel C (IM7/epoxy composite with a mat surface ply) during the second test series. During this cut the composite melted, suggesting frictional heating.

Mass concentration and emission rate results from the APS are summarized in Table 7. The aerosol generation by the band saw (when not cutting a panel) appeared to be minimal, as the concentration measured when the saw was operating without cutting was only 0.05 mg/m^3, versus a background concentration of 0.03 mg/m^3. The contribution of the band saw

is less than 2% of the mass concentration measured during the first test series. The emission rate results indicate that 10–20% of the material cut becomes airborne dust that is smaller than 20 μm. With the exception of panel C, which melted, less than 8% of the mass of aerosol generated is explained by FMPS measurements (i.e., of ultrafine particles). For panel C, however, almost 30% of the particle mass was attributed to ultrafine particles.

Table 8 summarizes number concentration and emission rates measured with the FMPS. In general, the number concentrations were between 1 x 10^5 and 7 x 10^5 particles/cm^3 during cutting. When the composite panel melted, the particle number concentration was nearly 1.57×10^6 particles/cm^3. In contrast, the ambient background and the concentration during the operation of the band saw were 1.1 and 1.3×10^4 particles/cm^3, respectively. Clearly, cutting the composite with the band saw creates a large number of particles smaller than 100 nm. Size-dependent aerosol emission rates are presented in Figures 8–11. Cutting panels with the band saw resulted in an aerosol with a mass distribution mode between 4 and 5 μm (Figures 8 and 9).

The particle number concentrations measured by the FMPS shifted during panel cutting. During the cutting of the first two panels, Panel A and Panel B, the emission rates had modes between 8 and 30 nm. During the remaining runs, the modes were between 40 and 50 nm. As shown in Figure 12, the mass fraction of the aerosol explained by the FMPS increased with run number until the band saw blade broke and was replaced. In this plot, runs 1–4 were from the first session, which involved multiple cuts, and runs 5–8 were from the second session, which involved single cuts. During run 7, the band saw blade broke and the test panel partially melted. For the first seven runs, run number explained 79.6% of the variability in log$_{10}$ (fraction of mass from the FMPS). Perhaps the blade was deteriorating and the cutting process grew hotter, increasing the aerosol generation caused by evaporation and condensation.

Table 7. Mass concentration measurements from APS and calculated mass emission rates from APS and FMPS.

Testing	Mass concentration, mg/m^3	Emission rate (including FMPS), mg of aerosol/cm^3 of cut	Fraction of mass emissions from FMPS	Mass fraction of respirable aerosol
Session 1, May 16				
Panel A	1.56	118.42	1.00×10^{-2}	0.55
Panel B	1.74	124.88	3.22×10^{-3}	0.58
Panel C	2.56	119.90	1.04×10^{-2}	0.54
Panel D	1.82	215.53	3.71×10^{-2}	0.54
Running band saw with no cutting	0.05	–	–	–
Background	0.03	–	–	–
Session 2, May 17				
Panel A	0.60	122.38	7.26×10^{-2}	0.57
Panel B	0.29	71.46	4.36×10^{-2}	0.46
Panel C	0.43	200.48	2.86×10^{-1}	0.78
Panel D	0.56	237.03	2.62×10^{-2}	0.58

Table 8. Particle number concentration and emission rates, as measured by FMPS, for cutting with the band saw.

Testing	Number concentration, particles/cm^3	Emission rate, particles/cm^3 of cut
Six or 12 cuts		
Panel A	3.45×10^5	2.95×10^{13}
Panel B	4.8×10^5	4.62×10^{13}
Panel C	7.3×10^5	3.59×10^{13}
Panel D	5.60×10^5	5.46×10^{13}
Running band saw with no cutting	1.52×10^4	–
Background	1.09×10^4	–
Single cut		
Panel A	5.33×10^5	1.39×10^{14}
Panel B	1.54×10^5	6.09×10^{13}
Panel C	1.58×10^6	6.72×10^{14}
Panel D	3.34×10^5	1.85×10^{14}
Background	1.28×10^4	–
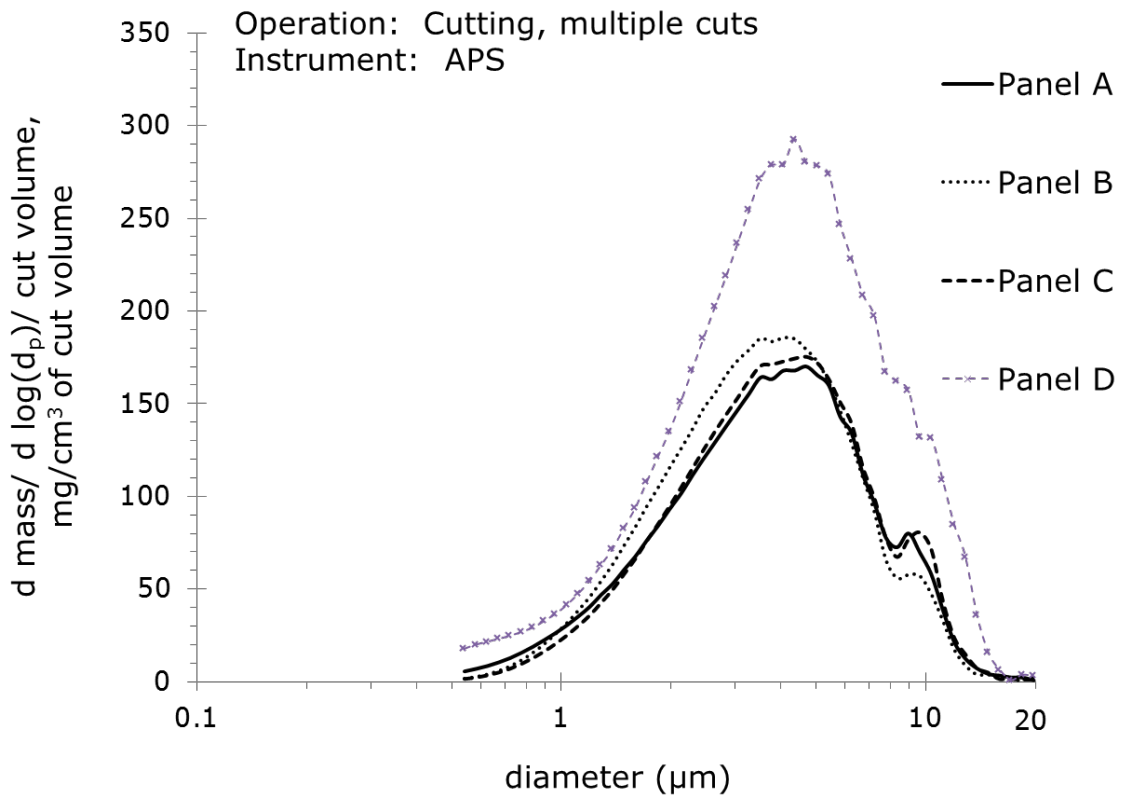
Figure 8. Mass emission rates as a function of particle diameter (d_p) from the first session with the band saw.
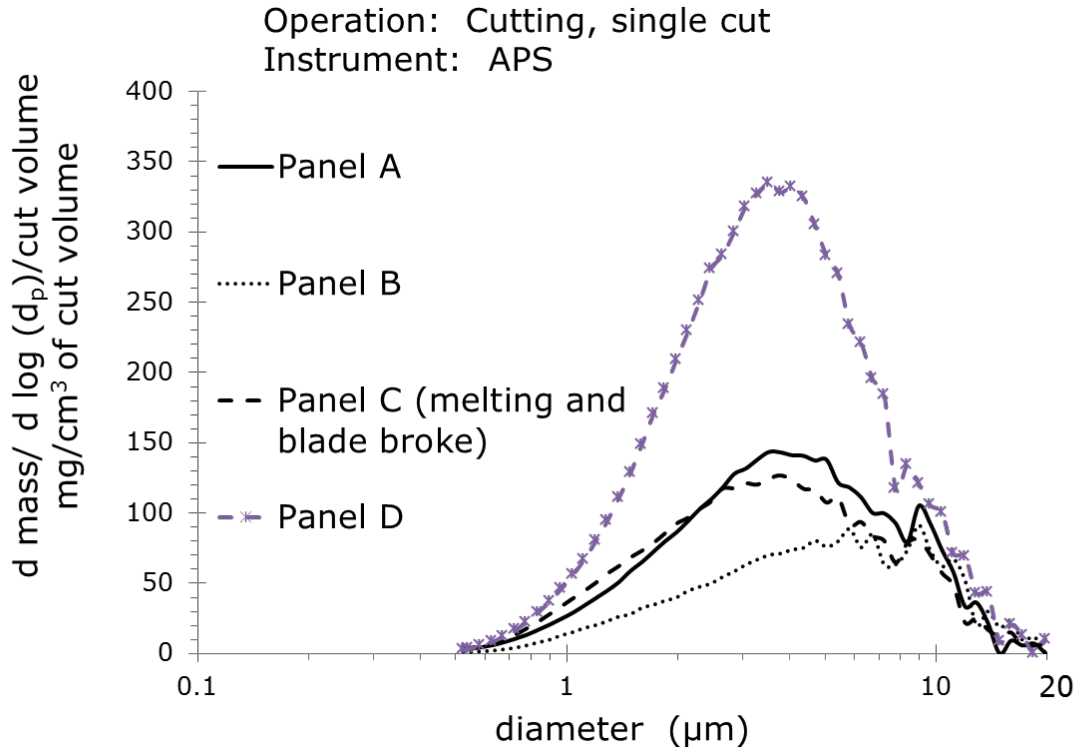
Figure 9. Mass emissions as a function of particle diameter (d_p) during the second session with the band saw.
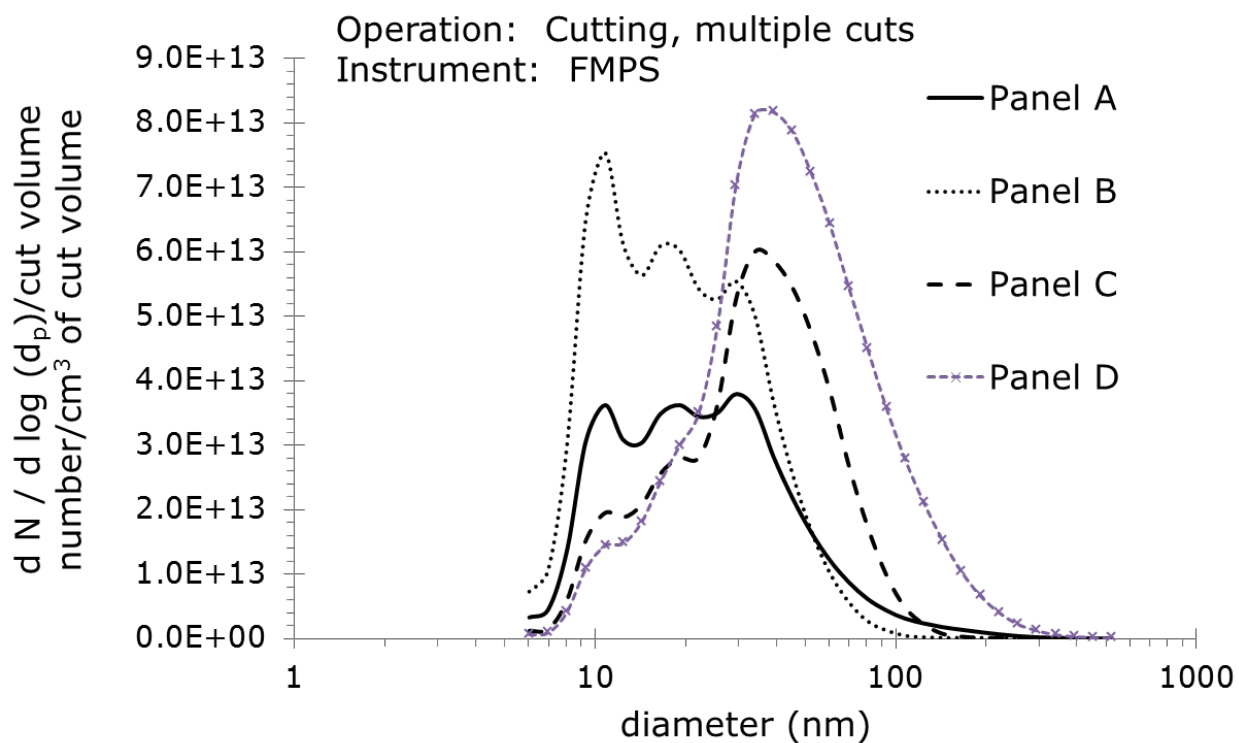
Figure 10. Particle number concentration as a function of particle diameter (d_p) measured with the FMPS involving multiple cuts. During the second two cuts there was a shift to a larger particle size.
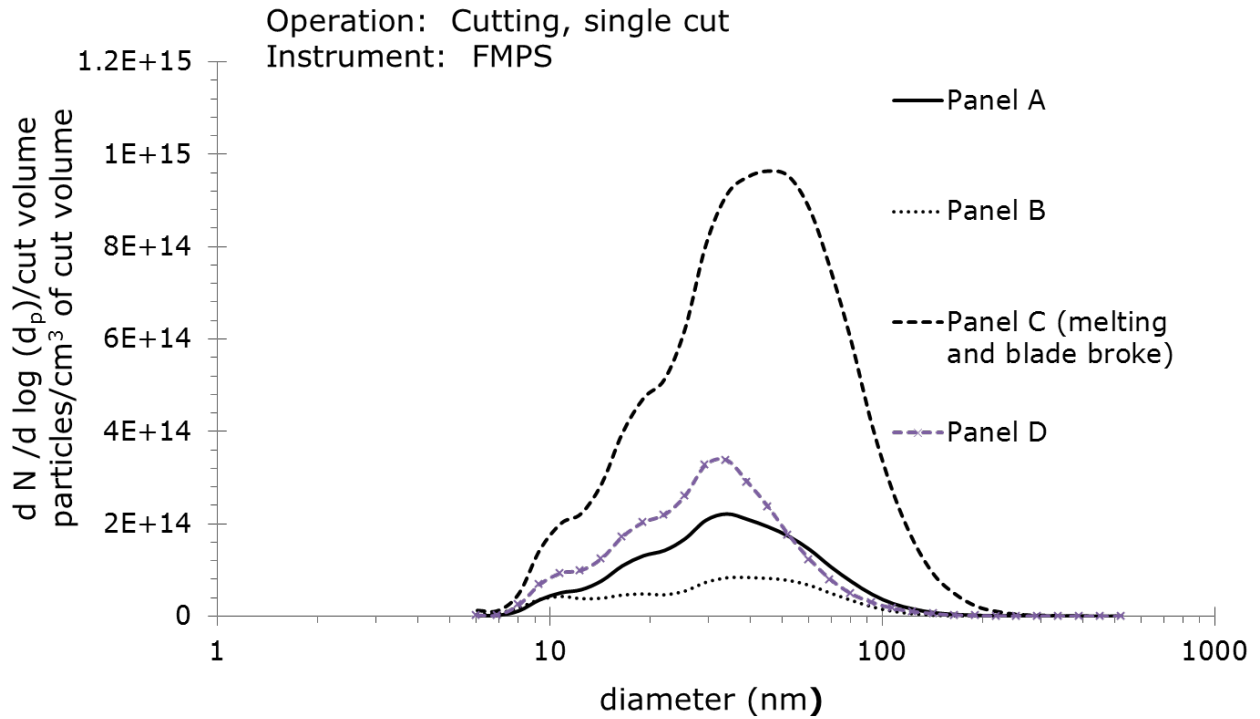
Figure 11. Particle emission rate as a function of particle diameter (d_p) measured with the FMPS during second cutting session. When panel C was cut, the saw blade broke and the composite panel partially melted.
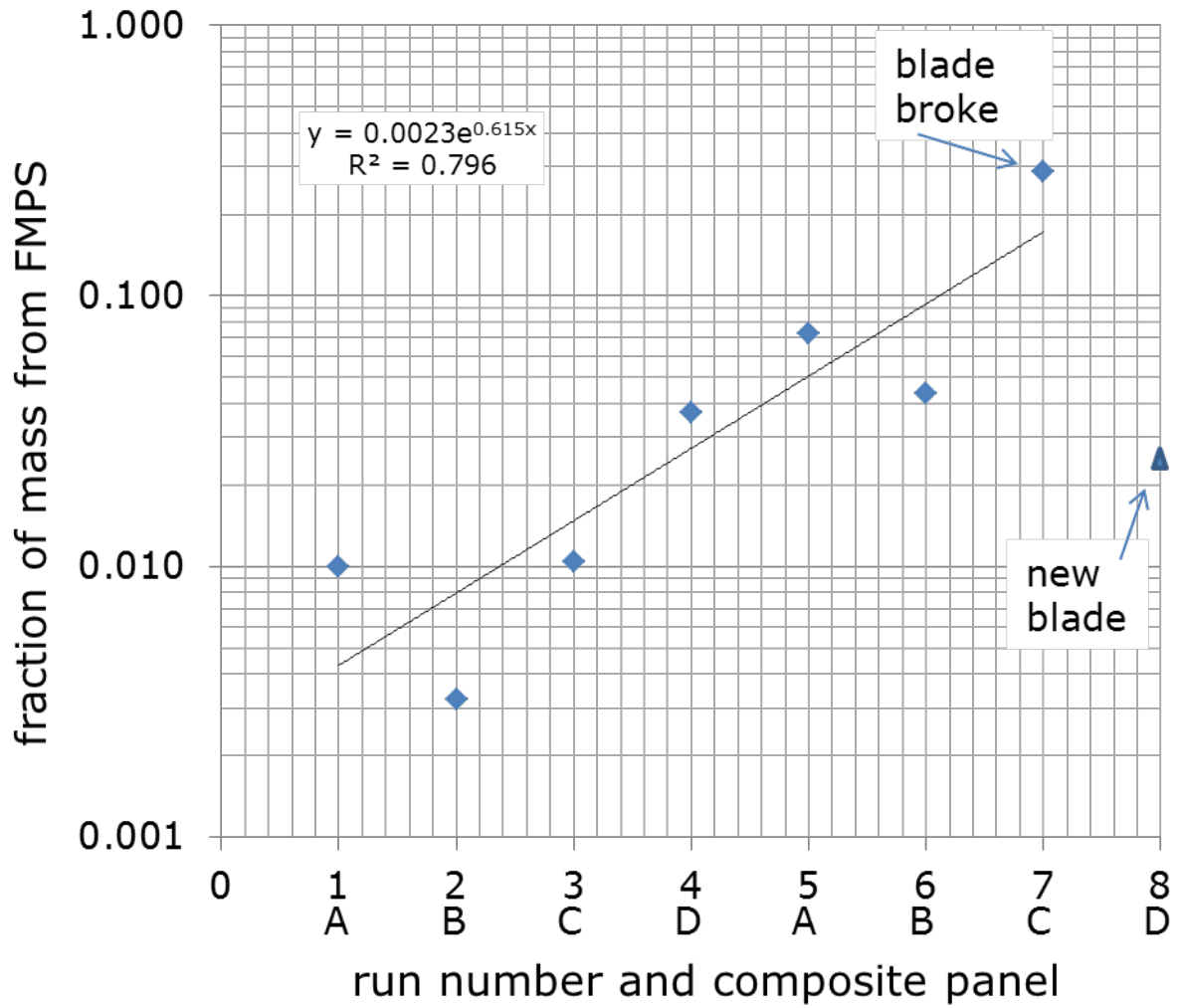
Figure 12. Fraction of mass from the FMPS appears to increase with run number for panel cutting with the band saw.

During cutting with the band saw, fibers or structures containing fibers were not detected on any of the samples collected for TEM. Thus, the fiber concentration is less than 0.2 fibers or structures containing fibers per cm^3 (the limit of detection). A typical electron microscopy grid is shown in Figure 13.
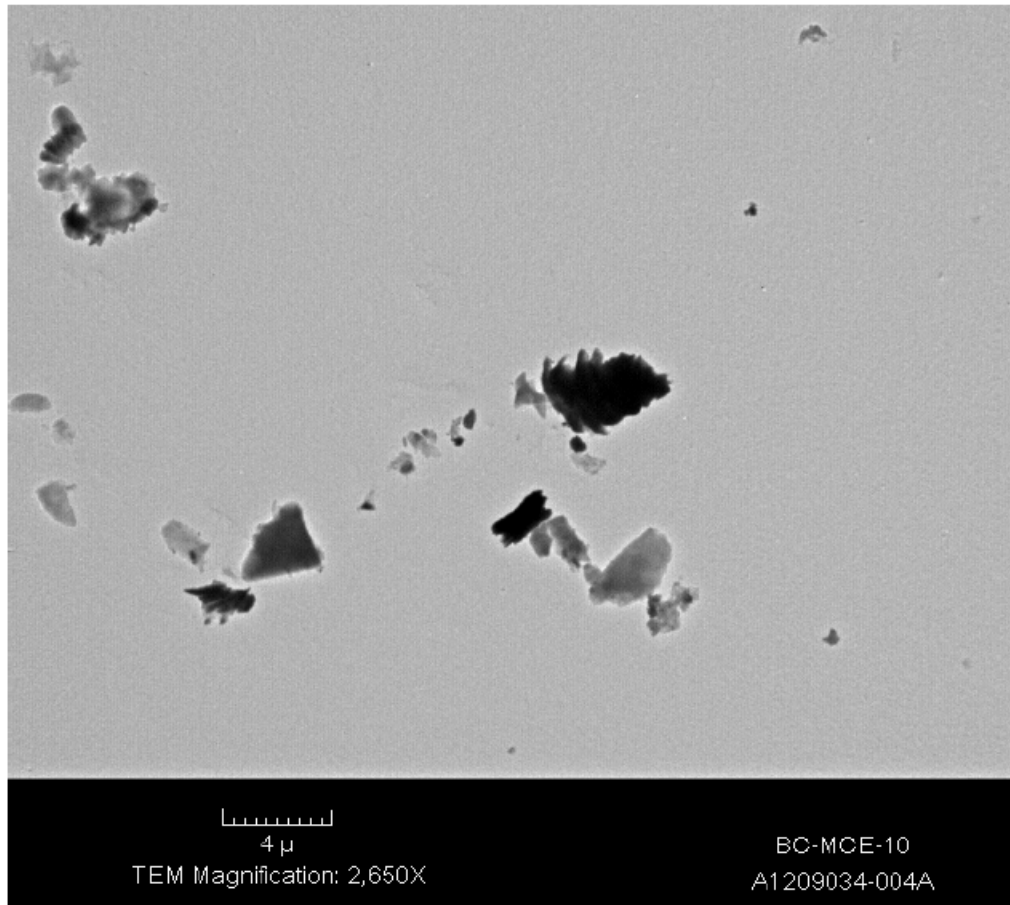
Figure 13. TEM image showing the absence of CNTs or fibers in sample collected in duct during the cutting of composite panel D.

Table 9 presents the elemental carbon concentrations measured during the first cutting session with the band saw. Elemental carbon on the worker was either undetected or in concentrations between the LOD and the LOQ, and less than those measured at the background location. In contrast, the elemental carbon concentrations measured in the duct were between 50 and

84 μg/m^3. This indicates that the ventilation system effectively captured the generated dust. The CNTs did not appear to elevate the elemental carbon concentrations. In Table 9, the elemental carbon emission rate for panel D is noticeably higher than the rates for panels C and D. Apparently, the elemental carbon emissions are largely explained by the graphite and carbon fibers in the test panels. Furthermore, fibers were not detected in the TEM samples collected during panel cutting. The graphite and carbon fibers in the composite are likely additional sources of elemental carbon that might overwhelm the contribution of the CNTs.

Table 9. Elemental carbon concentrations from cutting the composite with the band saw.

Test Panel	Elemental carbon concentration, (μg/m^3)			Elemental carbon emission rate, (mg of elemental carbon/cm^3 of cut volume)
	Worker	Source	Duct	
Panel B	0.3*	35	50	4.9
Panel C	0.8*	93	84	4.1
Panel D	< 0.7	54	75	6.9
Background	1.8	–	–	–

* – between the LOD and the LOQ.

Emissions from Composite Sanding

During the sanding of panel A, numerous experimental problems occurred, but the data for this panel are included for the sake of report completeness. Aerosol measurements made with the FMPS and APS are summarized in Table 10, Figure 14, and Figure 15. In Table 10, mass emission rate (see Equation 4) is largely determined by the mass concentration estimated from the APS. The mass concentrations and emission rates during two tests (panel C and panel D1 in Table 10) were at least a factor of 8 higher than

during other tests. The pressure that the worker applied to the sander was not controlled. Possibly, the pressure applied to the sander is causing the sander mass emissions to vary. This pressure or force is normal to the direction of sanding, and this affects the frictional force at the sander-composite interface [Gheerardyn et al. 2010; Ringlein and Robbins 2004].

The mass concentration from the sander was negligible as measured in the laboratory. As shown in Figure 15, the size distribution did not appear to vary with the composite being sanded. The modes appear to be between 3 and 4 μm.

In Table 10, the emission rate of ultrafine particles measured by the FMPS is between 10^9 and 4.3×10^9 particles/sec. The sander by itself produced an emission rate of 2×10^9 particles/sec. Thus, the sander's motor creates approximately 50% of the particles detected by the FMPS. As shown in Figure 14, the sander's motor probably explains much of the aerosol generation in the 6- to 30-nm sizes. These particles do not contribute to the mass of the aerosol generated. For particles larger than 30 nm, aerosol generation is clearly caused by sanding of the composite.

Table 10. Summary of aerosol measurements during sanding.

Testing	Mass concen-tration, mg/m^3, from APS	Mass emission rate, mg/sec	Mass fraction of respirable aerosol	Number concentration from FMPS, particles/sec	Number emission rate, particles/sec
Panel A	0.019	0.011	0.58	6.3E + 03	3.5E + 09
Panel B	0.078	0.040	0.60	5.6E + 03	3.0E + 09
Panel C	0.598	0.321	0.64	5.1E + 03	3.6E + 09
Panel D1	0.692	0.361	0.62	6.3E + 03	4.3E + 09
Panel D2	0.048	0.024	0.58	1.9E + 03	1.0E + 09
Running sander in lab without sanding	0.002	0.001	–	4.5E + 03	2.1E + 09
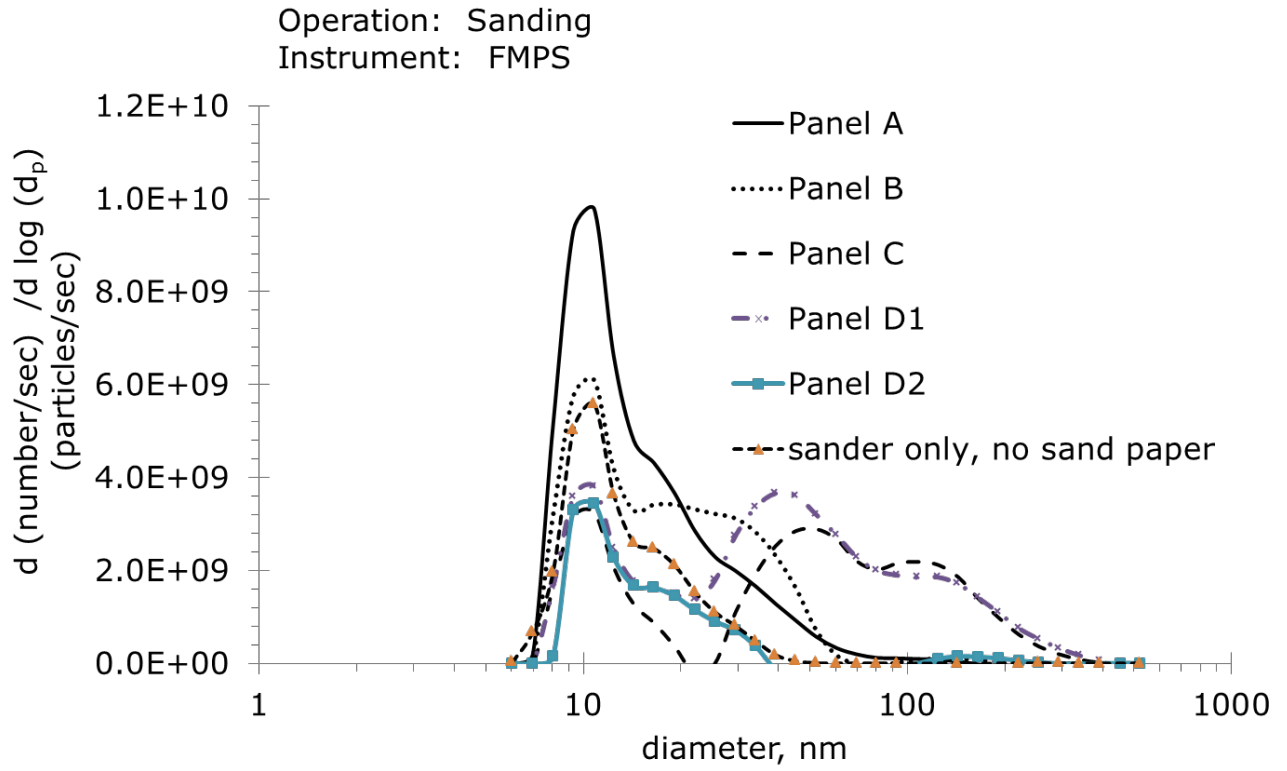
Figure 14. Size-dependent particle number emission rates as a function of particle diameter (d_p) measured with FMPS.
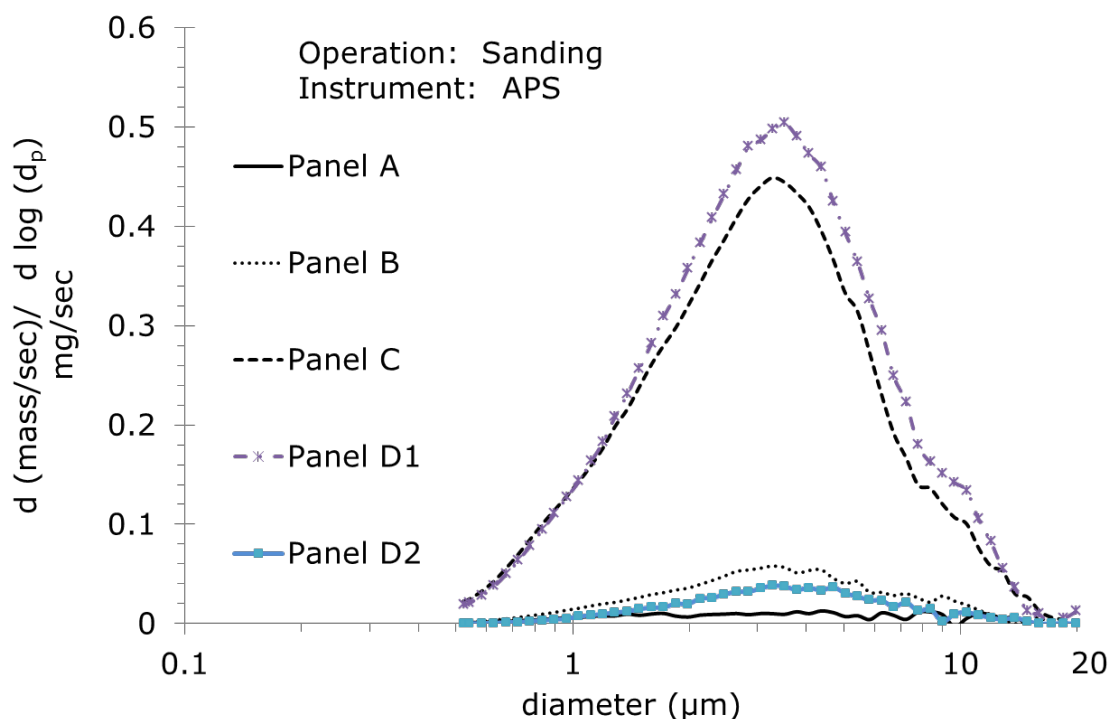
Figure 15. Size-dependent mass emission rates as a function of particle diameter (d_p) measured with the APS during sanding.

Table 11 presents fiber concentrations and emission rates for the composite panels that were sanded. Fibers were not detected on the personal samples. During the sanding of panels A, B, and C, fibers or structures with exposed fibers were not detected on the background sample, in the duct, or on the worker. When composite panel D (IM7/epoxy with nano-coated mat surface ply) was sanded, detectable fiber concentrations were measured in the duct and behind the sanding operation (i.e., the source sample). As shown in Figure 16−Figure 18, individual fibers and fibers protruding from individual particles were observed. These fibers appear to have diameters between 50 and 200 nm. In addition, the fibers appear to be less than 10 μm long.

Table 11. Fiber concentrations and emissions generated during composite sanding.

Testing	Fiber concentration, fibers/cm^3		Fiber emission rate, fibers/sec
	Source	Duct	–
Panel A	ND	ND	–
Panel B	1 fiber detected	ND	–
Panel C	1 fiber detected	ND	–
Panel D1	270	290	1.91×10^8
Panel D2	11	4.3	2.83×10^6

ND = less than 0.2 fibers/cm^3.
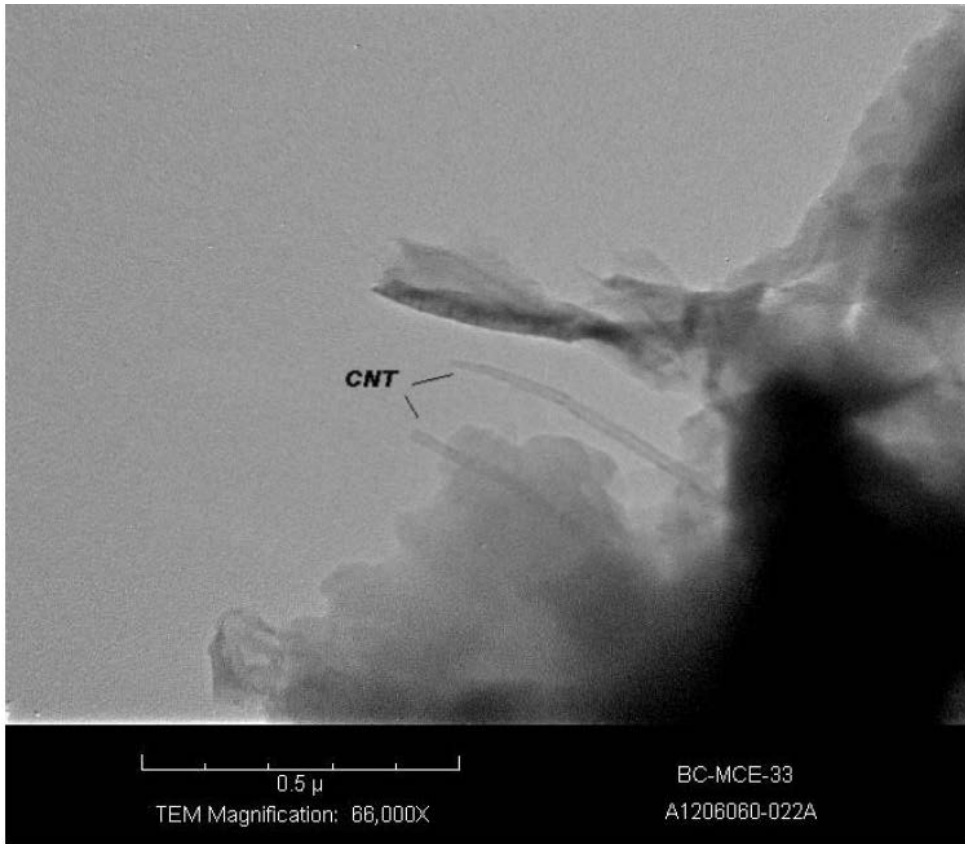
Figure 16. Fiber protruding from debris collected on filter just downstream of the band saw's table during sanding on panel D1.
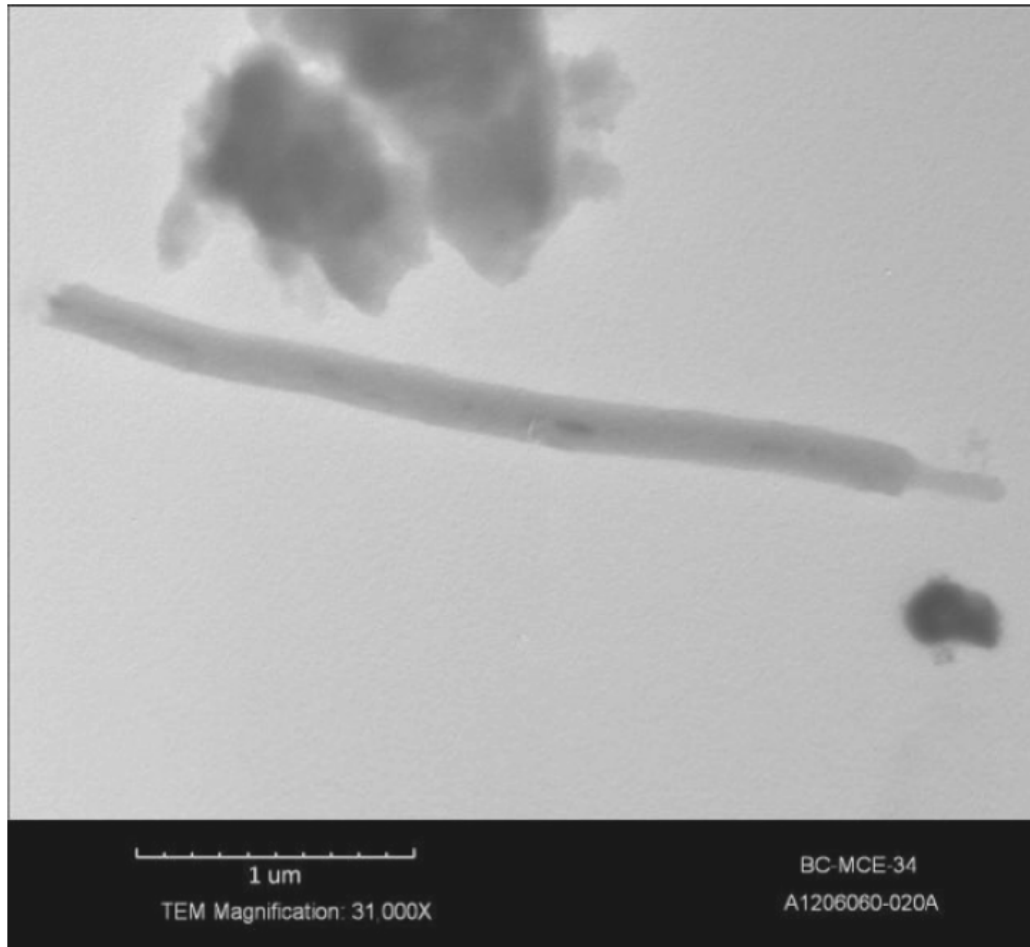
Figure 17. Individual fiber from duct sample collected during sanding of panel D1.
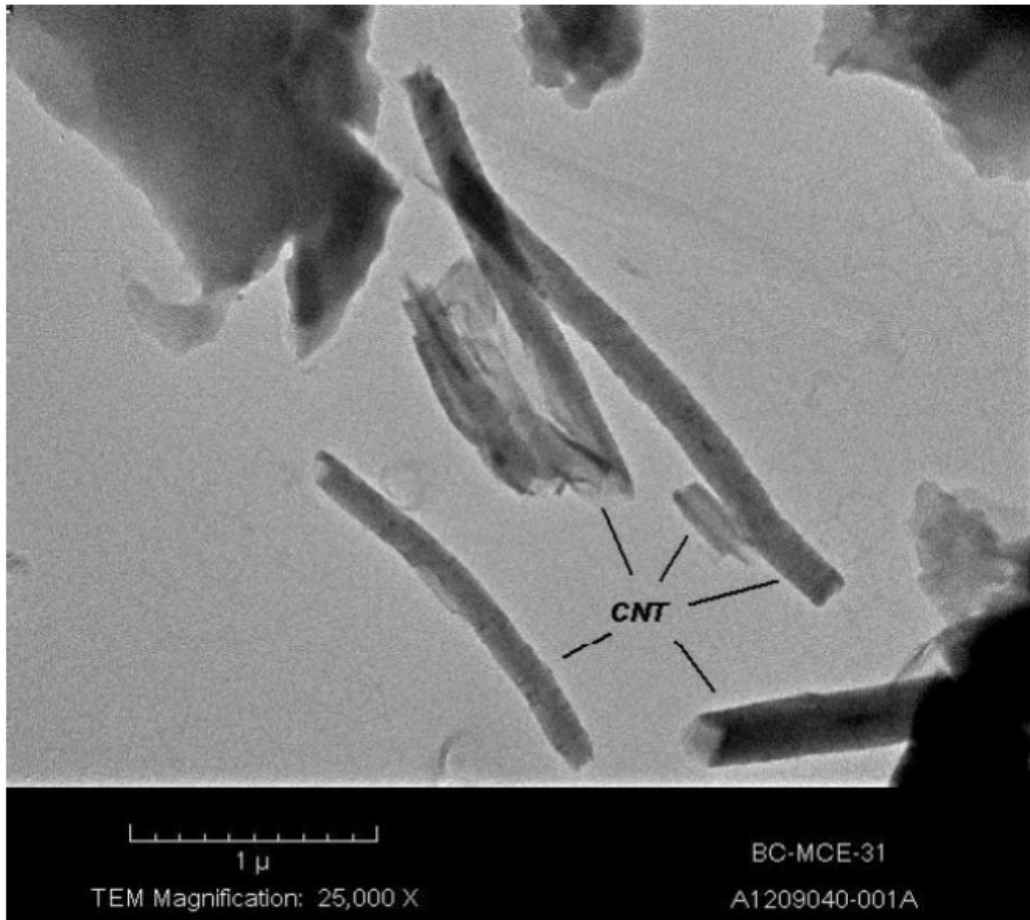
Figure 18. Individual CNTs collected at source for panel D1.

Table 12 lists the elemental carbon concentrations measured during the sanding operations. The concentrations were measured on the worker, just downstream of the sanding operation, and in the duct. A background sample collected for elemental carbon during all of the sanding and cutting operations on May 17 indicated that the background concentration was 0.1 µg/m^3. This concentration was measured behind the enclosure, some 30 feet from the negative air machine. Because the composites all contained graphite, elemental carbon concentrations are not necessarily caused by CNTs. During sanding, the elemental carbon concentrations measured on the worker were between <0.5 µg/m^3 and 1.6 µg/m^3. Sanding of the composite panels caused emissions of elemental carbon, because the concentrations measured at the source and in the duct are generally higher than the concentrations measured on the worker. However, sanding of panels containing the CNTs did not generate much higher concentrations than other cases during work on panels without nanomaterials that contained graphite fibers. This indicates that the primary contribution to the elemental carbon emissions was graphite fiber and not unbound CNTs. However, a relatively large number of fibers were observed during sanding on panels D1 and D2, which contained a CNT-coated mat.

Table 12. Elemental carbon concentrations and emission rates measured during sanding of composite panels.

Testing	Elemental carbon concentration, µg/m^3			Emission rate, µg/sec
	Worker	Source	Duct	
Panel A	0.30*	2.33	0.64*	0.89*
Panel B	0.80*	15.58	2.95	1.63
Panel C	1.62	2.69	<0.4	<0.22
Panel D1	<0.5	7.50	3.85	2.51
Panel D2	<0.5	<0.5	0.70*	0.39*
Background concentration during day	0.1			–

*Between the LOD (0.2 µg/filter) and the LOQ (0.52 µg/filter) for elemental carbon.

Conclusions and Recommendations

Discussion

The available data generally support the conclusion that the hood efficiently captured the debris generated by cutting and sanding the composite panels. Qualitative flow visualization suggested that the ventilation system was separating the worker from the aerosol generated within the hood. For cutting the composite panels multiple times, the elemental carbon concentrations measured on the worker were 1% of the concentration measured in the duct (Table 9), and the worker exposure to elemental carbon was consistent with ambient air pollution [Yu et al. 2004]. During sanding operations, fiber concentrations (Table 11) were below the LOD of 0.2 fibers/cm^3 on the worker. In the duct, fiber concentrations were 290 (panel D1) and 4.3 (panel D2) fibers/cm^3, indicating worker exposure was less than 5% of the concentration measured in the duct. However, the

elemental carbon concentrations measured during sanding (Table 12) did not result in a large difference between the concentration measured on the worker and the in-duct concentrations. Also, all of the concentrations reported in Table 12 are consistent with ambient air pollution [Yu et al. 2004]. Perhaps the elemental carbon emission rate for the sanding task was too low to evaluate the ability of the hood to contain the emissions during sanding.

For suggested exposure limits for engineered nanomaterials listed in Table 1, an evaluation as to whether exposure measurements are due to engineered nanomaterials or extraneous aerosol sources is recommended [Van Broekhuizen et al. 2012]. The study results confirm this recommendation. When CNTs were identified by TEM, the number concentrations during sanding were 4.3 and 290 fibers or structures containing fibers/cm^3 (see Table 11). In contrast, the number concentration of aerosol generated by the sander was about 4.5 x 10^3 particles/cm^3, which was largely caused by the sander's motor. Furthermore, the fiber concentration was much smaller than the number concentration measured by FMPS, reported in Table 8 and Table 10. Although number concentrations generated during band saw cutting were 10^5 to 10^6 particles/cm^3 (Table 8) and elemental carbon concentrations were 50 to 84 μg/m^3 (Table 9), TEM did not reveal the presence of CNTs or any fibers. The lack of detected fibers during the band saw cutting of panel D is consistent with earlier results [Bello et al. 2009].

The elemental carbon emissions listed in Table 9 and Table 12 are not respirable elemental carbon emissions. However, the respirable fraction of the aerosol was between 46% and 78% (see Table 7 and Table 10). Possibly, the graphite fibers in the composite would affect the measurement of respirable elemental carbon used to assess exposure to CNTs.

The cutting operation may have generated significant frictional heating as the composite panel melted during one test, and the estimated mass of aerosol from the FMPS appears to increase exponentially with run number (Figure 12). Perhaps frictional heating caused aerosol generation by evaporation/condensation phenomena, resulting in very high number concentrations measured by the FMPS. This possibility needs to be considered in future studies.

Recommendations

The band saw used in this study had an exhaust take-off that could be attached to a vacuum cleaner. However, air flow recommendations are not available. Clearly, the hood used in this study effectively contained the emissions, but this enclosure may not be suitable in all applications. Local exhaust ventilation can be used to capture and collect the aerosol and debris generated by the band saw. The ACGIH Ventilation Manual has ventilation recommendations for band saws [ACGIH 2010].

Sanding the composite panel D, which contained CNTs, generated measurable concentrations of fibers or fiber-containing structures. The extent of the hazard is not known, because relevant exposure metrics have not been developed. Careful and aggressive control of exposure to CNTs is recommended [Castranova et al. 2012]. Orbital sanders frequently have exhaust take-offs for drawing air through holes in the sanding pads and sandpaper. For orbital sanders, an exhaust flow rate of 30–40 cfm can provide a 90% reduction in emissions when an appropriate vacuum cleaner is used to provide airflow and collect dust [Thorpe and Brown 1994, 1995]. The dust collection bags provided with sanders may be ineffective as dust control measures. Vacuum cleaners can provide airflow and air cleaning, but their air flow must be maintained. Some vacuum cleaners lose noticeable amounts of air flow as debris accumulates on the filters [Heitbrink and Santalla-Elias 2009]. A cyclone can be used to capture most of the debris upstream of the vacuum cleaner's filters. In this way, the filter pressure loss does not increase greatly and airflow is maintained. These emissions could probably be controlled by either a conventional local exhaust ventilation hood or a high-velocity, low-volume ventilation system.

Process-related sources of elemental carbon include carbon brushes in electrical motors, as well as graphite and carbon fibers in composites. Particle number concentrations also appear to be a poor measure of exposure to the manufactured nanomaterials at this site, as the sawing operations generate very high number concentrations even without the use of engineered nanomaterials (Table 8).

References

ACGIH [2007]. Industrial Ventilation - A Manual of Recommended Practice for Operation and Maintenance. Cincinnati Ohio American Conference of Governmental Industrial Hygienists.

ACGIH [2010]. Industrial ventilation: a manual of recommended practice for design Cincinnati, Ohio: American Conference of Governmental Industrial Hygienists

ACGIH [2012]. TLVs and BEIs: threshold limit values for chemical substances and physical agents and biological exposure indices. Cincinnati, OH: American Conference of Governmental Industrial Hygienists.

Bayer MaterialScience [2010]. Occupational exposure limit (OEL) for Baytubes defined by Bayer MaterialScience. Leverkusen, Germany: Bayer MaterialScience.

Bello D, Hart AJ, Ahn K, Hallock M, Yamamoto N, Garcia EJ, Ellenbecker MJ, Wardle BL [2008]. Particle exposure levels during CVD growth and subsequent handling of vertically-aligned carbon nanotube films. Carbon *46*(6):974-977.

Bello D, Wardle B, Zhang J, Yamamoto N, Santeufemio C, Hallock M, Virji MA [2010]. Characterization of exposures to nanoscale particles and fibers during solid core drilling of hybrid carbon nanotube advanced composites. International journal of occupational and environmental health *16*(4):434-450.

Bello D, Wardle BL, Yamamoto N, Guzman deVilloria R, Garcia EJ, Hart AJ, Ahn K, Ellenbecker MJ, Hallock M [2009]. Exposure to nanoscale particles and fibers during machining of hybrid advanced composites containing carbon nanotubes. Journal of Nanoparticle Research *11*(1):231-249.

Brockman J [2001]. Sampling and Transport of Aerosols. In: PA Baron KW, ed. Aerosol Measurement Principles, Techniques, and Applications. 2nd. Hoboken, New Jersey: Wiley-Interscience, pp. 143-196

Buzea C, Blandino IIP, Robbie K [2007]. Nanomaterials and nanoparticles: sources and toxicity. Biointerphases *2* (4):MR17-MR172.

Castranova V, Schulte PA, Zumwalde RD [2012]. Occupational nanosafety considerations for carbon nanotubes and carbon nanofibers. Accounts of Chemical Research.

Cena LG, Peters TM [2011]. Characterization and control of airborne particles emitted during production of epoxy/carbon nanotube nanocomposites. Journal of occupational and environmental hygiene *8*(2):86-92.

Chang CS, Ho JE, Chan CH, Hwang BC [2011]. Prediction of Cutting Temperatures in Turning Carbon Fiber Reinforced Plastics Composites with Worn Tools. Journal of Applied Sciences *11*:3698-3707.

Chen WC [1997]. Some experimental investigations in the drilling of carbon fiber-reinforced plastic (CFRP) composite laminates. International Journal of Machine Tools and Manufacture *37*(8):1097-1108.

Chen X, Wang J, Lin M, Zhong W, Feng T, Chen X, Chen J, Xue F [2008]. Mechanical and thermal properties of epoxy nanocomposites reinforced with amino-functionalized multi-walled carbon nanotubes. Materials Science and Engineering: A *492*(1):236-242.

European Agency for Safety and Health at Work [2009]. Literature review: workplace exposure to nanoparticles.89 pages.

Evans DE, Ku BK, Birch ME, Dunn KH [2010]. Aerosol monitoring during carbon nanofiber production: mobile direct-reading sampling. Annals of Occupational Hygiene *54*(5):514-531.

Gheerardyn L, Le Bihan O, Dore E, Morgeneyer M [2010]. Nanoparticle release from nano-containing product, introduction to an energetic approach.

Ham S, Yoon C, Lee E, Lee K, Park D, Chung E, Kim P, Lee B [2012]. Task-based exposure assessment of nanoparticles in the workplace. Journal of Nanoparticle Research *14*(9):1-17.

Hampl V, Niemelä R, Shulman S, DAVID LB [1986]. Use of Tracer Gas Technique for Industrial Exhaust Hood Efficiency Evaluation–Where to Sample? The American Industrial Hygiene Association Journal *47*(5):281-287.

Han SG, Andrews R, Gairola CG [2010]. Acute pulmonary response of mice to multi-wall carbon nanotubes. Inhalation toxicology *22*(4):340-347.

Heitbrink WA, Collingwood S [2005]. Aerosol generation by blower motors as a bias in assessing aerosol penetration into cabin filtration systems. Journal of occupational and environmental hygiene *2*(1):45-53.

Heitbrink WA, Santalla-Elias J [2009]. The effect of debris accumulation on and filter resistance to airflow for four commercially available vacuum cleaners. Journal of occupational and environmental hygiene *6*(6):374-384.

Hsieh YC, Chou YC, Lin CP, Hsieh TF, Shu CM [2010]. Thermal analysis of multi-walled carbon nanotubes by Kissinger's corrected kinetic equation. Aerosol and Air Quality Research *10*(3):212-218.

Hubbs A, Castranova V, Ma J, Frazer D, Siegel P, Ducatman B, Grote A, Schwegler-Berry D, Robinson V, Van Dyke C [1997]. Acute lung injury induced by a commercial leather conditioner. Toxicology and Applied Pharmacology *143*(1):37-46.

ISO [2008]. Nanotechnologies -- Health and safety practices in occupational settings relevant to nanotechnologies. International Organization for Standardization.

Kisin E, Murray A, Sargent L [2010]. Pulmonary response, oxidative stress and genotoxicity induced by carbon nanofibers. Toxicologist *114*(1):169.

Koponen I, Jensen K, Schneider T [2009]. Sanding dust from nanoparticle-containing paints: physical characterisation.

Kuhlbusch T, Asbach C, Fissan H, Göhler D, STINZT M [2011]. Nanoparticle exposure at nanotechnology workplaces: a review. Particle and Fibre Toxicology *8*(1):22.

Lee T, Kim SW, Chisholm WP, Slaven J, Harper M [2010]. Performance of high flow rate samplers for respirable particle collection. Annals of Occupational Hygiene *54*(6):697-709.

Malkin S, Guo C [2007]. Thermal analysis of grinding. CIRP Annals-Manufacturing Technology *56*(2):760-782.

Mark D [2007]. Occupational exposure to nanoparticles and nanotubes. In: Hester RE, Harrison RM, eds. Nanotechnology: consequences for human health and the environment. RSC Publishing, pp. 50-80

McShane H, Arafat ES, McLaughlin P, Cochran R, Miller K [1999]. Heat Damage Assessment for Naval Aircraft Composites. DTIC Document.

Methner M, Crawford C, Geraci C [2012]. Evaluation of the Potential Airborne Release of Carbon Nanofibers During the Preparation, Grinding, and Cutting of Epoxy-Based Nanocomposite Material. Journal of occupational and environmental hygiene *9*(5):308-318.

Methner M, Hodson L, Dames A, Geraci C [2009]. Nanoparticle emission assessment technique (NEAT) for the identification and measurement of

potential inhalation exposure to engineered nanomaterials—Part B: Results from 12 field studies. Journal of occupational and environmental hygiene *7*(3):163-176.

Methner MM, Birch ME, Evans DE, Ku BK, Crouch K, Hoover MD [2007]. Identification and characterization of potential sources of worker exposure to carbon nanofibers during polymer composite laboratory operations. Journal of occupational and environmental hygiene *4*(12):125-130.

Morawska L, Ristovski Z, Jayaratne E, Keogh DU, Ling X [2008]. Ambient nano and ultrafine particles from motor vehicle emissions: Characteristics, ambient processing and implications on human exposure. Atmospheric Environment *42*(35):8113-8138.

Murashov V, Howard J [2011]. Health and safety standards. In: Nanotechnology Standards. New York: pp. 209-238

Nagai H, Okazaki Y, Chew SH, Misawa N, Yamashita Y, Akatsuka S, Ishihara T, Yamashita K, Yoshikawa Y, Yasui H [2011]. Diameter and rigidity of multiwalled carbon nanotubes are critical factors in mesothelial injury and carcinogenesis. Proceedings of the National Academy of Sciences *108*(49):E1330-E1338.

Nanocyl [2009]. Resonsible care and nanomaterials case study European Responsible Care Conference, Prague, October, 2009.

NIOSH [1994]. NIOSH manual of analytical methods (NMAM) Method 7402: asbestos by TEM. Cincinnati, OH: U.S. Department of Health and Human Services, National Institute for Occupational Safety and Health.

NIOSH [2003]. NIOSH manual of analytical methods (NMAM) Method 5040: elemental carbon (diesel particulate). Cincinnati, OH: U.S. Department of Health and Human Services, National Institute for Occupational Safety and Health.

NIOSH [2013]. NIOSH Current Intelligence Bulletin 65: occupational exposure to carbon nanotubes and nanofibers. Cincinnati, OH: Department of Health and human Services, Centers for Disease Control and Prevention, National for Occupational Safety and Health. Publication No. DHHS (NIOSH) Publication No. 2013-145.

Occupational Safety and Health Adminstration [2013]. Working Safely with Nanomaterials. [http://www.osha.gov/Publications/OSHA_FS-3634.pdf]

Pauluhn J [2010]. Subchronic 13-week inhalation exposure of rats to multiwalled carbon nanotubes: toxic effects are determined by density of agglomerate structures, not fibrillar structures. Toxicological Sciences *113*(1):226-242.

Porter DW, Hubbs AF, Mercer RR, Wu N, Wolfarth MG, Sriram K, Leonard S, Battelli L, Schwegler-Berry D, Friend S [2010]. Mouse pulmonary dose-and time course-responses induced by exposure to multi-walled carbon nanotubes. Toxicology *269*(2-3):136-147.

Ringlein J, Robbins MO [2004]. Understanding and illustrating the atomic origins of friction. American journal of physics *72*:884.

Safe Work Australia [2009a]. Engineered nanomaterials: a review of the toxicology and health hazards.163 pages.

Safe Work Australia [2009b]. Engineered Nanomaterials: Evidence on the Effectiveness of Workplace Controls to Prevent Exposure.75 pages.

Schlagenhauf L, Chu B, Buha J, Nüesch FA, Wang J [2012]. Release of carbon nanotubes from an epoxy-based nanocomposite during an abrasion process. Environmental Science & Technology.

Shi JP, Evans DE, Khan AA, Harrison RM [2001]. Sources and concentration of nanoparticles (<10nm diameter) in the urban atmosphere. Atmospheric Environment *35*(7):1193-1202.

Shvedova AA, Kisin ER, Mercer R, Murray AR, Johnson VJ, Potapovich AI, Tyurina YY, Gorelik O, Arepalli S, Schwegler-Berry D [2005]. Unusual inflammatory and fibrogenic pulmonary responses to single-walled carbon nanotubes in mice. American Journal of Physiology-Lung Cellular and Molecular Physiology *289*(5):L698-L708.

Stabile L, Ruggiero A, Iannitti G, Buonanno G [2012]. Generation of ultrafine particles by high-velocity impact of metal projectiles on a metallic target. Journal of aerosol science.

Stanier CO, Khlystov AY, Pandis SN [2004]. Ambient aerosol size distributions and number concentrations measured during the Pittsburgh Air Quality Study (PAQS). Atmospheric Environment *38*(20):3275-3284.

Szymczak W, Menzel N, Keck L [2007]. Emission of ultrafine copper particles by universal motors controlled by phase angle modulation. Journal of aerosol science *38*(5):520-531.

Thorpe A, Brown R [1994]. Measurements of the effectiveness of dust extraction systems of hand sanders used on wood. Annals of Occupational Hygiene *38*(3):279-302.

Thorpe A, Brown R [1995]. An improved design for the dust extraction system of orbital sanders used on wood. Annals of Occupational Hygiene *39*(2):155-165.

Traceski FT [1999]. Assessing industrial capabilities for carbon fiber production. DTIC Document, OFFICE OF THE UNDER SECRETARY OF DEFENSE (ACQUISITION AND TECHNOLOGY) WASHINGTON DC.

Trakumas S, Willeke K, Grinshpun SA, Reponen T, Mainelis G, Friedman W [2001]. Particle emission characteristics of filter-equipped vacuum cleaners. AIHAJ-American Industrial Hygiene Association *62*(4):482-493.

Tsai SJ, Hofmann M, Hallock M, Ada E, Kong J, Ellenbecker M [2009]. Characterization and evaluation of nanoparticle release during the synthesis of single-walled and multiwalled carbon nanotubes by chemical vapor deposition. Environmental Science & Technology *43*(15):6017-6023.

Van Broekhuizen P, Van Veelen W, Streeekstra WH, Schulte P, Reijners L [2012]. Exposure Limits for Nanoparticles: Report of an International Workshop on Nano Reference Values. Annals of Occupational Hygiene *56*(5):515-524.

Van Broekhuizen P, Dorbeck-Jung B [2012]. Exposure Limit Values for Nanomaterials-Capacity and Willingness of Users to Apply a Precautionary Approach. Journal of Occupational and Environmental Hygiene

Weinert K, Kempmann C [2004]. Cutting temperatures and their effects on the machining behaviour in drilling reinforced plastic composites. Advanced Engineering Materials *6*(8):684-689.

Yu S, Dennis RL, Bhave PV, Eder BK [2004]. Primary and secondary organic aerosols over the United States: estimates on the basis of observed organic carbon (OC) and elemental carbon (EC), and air quality modeled primary OC/EC ratios. Atmos Environ *38*:5257-5268.

Zimmer M, Cheng Q, Li S, Brooks J, Liang R, Wang B, Zhang C [2012]. Comparative Characterization of Multiscale Carbon Fiber Composite with Long and Short MWCNTs at Higher Weight Fractions. Journal of Nanomaterials *2012*.

Acknowledgments

Delivering on the Nation's promise: Safety and health at work for all people through research and prevention.

To receive NIOSH documents or other information about occupational safety and health topics, contact NIOSH at

Telephone: 1-800- 232-4636

TTY: 1-888-232-6348

Web site: www.cdc.gov/info

For a monthly update on news at NIOSH, subscribe to NIOSH eNews by visiting www.cdc.gov/niosh/eNews.

SAFER • HEALTHIER • PEOPLE